AN INVESTIGATION OF

THE RADIOACTIVE ISOTOPES PRODUCED BY He^3

BOMBARDMENT OF Sm^{147} AND Gd^{152}

DISSERTATION

Presented in Partial Fulfillment of the Requirements for
the Degree Doctor of Philosophy in the
Graduate School of the Ohio State University

BY

RAYMOND HAL KELLEY, B.S., M. Sc.

******

THE OHIO STATE UNIVERSITY
1963

Approved by

M. L. Pool

Adviser
Department of Physics and
Astronomy

ACKNOWLEDGMENTS

I wish to express my gratitude and appreciation to my adviser, Professor Pool, for the extensive assistance, guidance, and cooperation he extended to me while I was engaged in this work. Mr. Harry G. Miller of the Gamma Spectroscopy group, by his assistance in the accumulation of data, gave me significant support at a critical time. To the other members of the Gamma Spectroscopy Group, I extend my warmest gratitude for the suggestions and the support which aided me in solving many harassing problems. And to the members of the O.S.U. cyclotron staff, in particular Dr. Ploughe and Mr. Weiler, my thanks for the effort they extended to make possible the bombardments I needed.

CONTENTS

TABLES

ILLUSTRATIONS

I. INTRODUCTION

In this investigation isotopically enriched samples of Samarium and Gadolinium were bombarded with He^3 nuclei. Even with bombarding energies of a few MeV at least six reaction channels have a probability of occurrence: (He^3,T), (He^3,d), (He^3,p), (He^3,n), $(He^3,2n)$, and $(He^3,3n)$. While this complicates the analysis of the experimental data it has two advantages over proton bombardment. First, it is possible to produce radioactive nuclei which cannot be produced by low energy proton bombardment and the radioactive nuclei produced can be assigned atomic number and mass number with a higher degree of certainty than with high energy proton bombardment (spallation reaction products). Secondly, the relative reaction cross sections for the reaction channels occurring can, in principle, be easily calculated. Thus the specific purpose of this experimental investigation was to study the radioactivity produced in the rare earth isotopes Sm^{147} and Gd^{152} with these objectives:

1. To attempt to identify the radioactive nuclei produced and the associated decay scheme of each nucleus.
2. To compare the experimental data and the conclusions therefrom with previously reported investigations.
3. To calculate the relative cross sections for the He^3 induced reactions for those radioactive nuclei whose decay schemes (levels and intensities) were known or deducible.

The subsequent sections in this paper consider the experimental procedure and apparatus used in this investigation, the experimental results and the conclusions drawn for each bombarded nuclei, and finally an evaluation of the investigation.

II. EXPERIMENTAL PROCEDURES

Stable isotopes enriched in Gd^{152} and Sm^{147} were bombarded with 16.5 MeV He^3 nuclei in the Ohio State University Cyclotron. Energy, half-lives, and coincidence data were measured for the radiations produced using scintillation counters and a solid state charged particle detector in conjunction with multi-channel pulse height analyzers. The details of the isotopic composition, sample preparation and handling, and the experimental apparatus are discussed in the following paragraphs.

1. ISOTOPIC COMPOSITION OF THE BOMBARDED SAMPLES

The isotopes of Gd^{152} and Sm^{147} were obtained from the Stable Isotopes Division of Oak Ridge National Laboratory, Oak Ridge, Tennessee. The composition and impurity content of these two isotopes are given in Table 1.

2. SAMPLE PREPARATION FOR BOMBARDMENT

The samples were placed in aluminum holders (see Plate I, Figure 1) which could be attached to the target assembly of the Ohio State University Cyclotron. To prepare a sample for bombardment approximately 6 mg of compound was spread uniformly over the bottom of the 9/16"x1/16" slit in the holder. Then a die was inserted in the slit and the powder compressed with a hydraulic press. After compression the compound covered the bottom of the slit uniformly and presented a smooth hard surface. The sample thickness was of the order of $10 mg/cm^2$.

PLATE I
SAMPLE HOLDERS

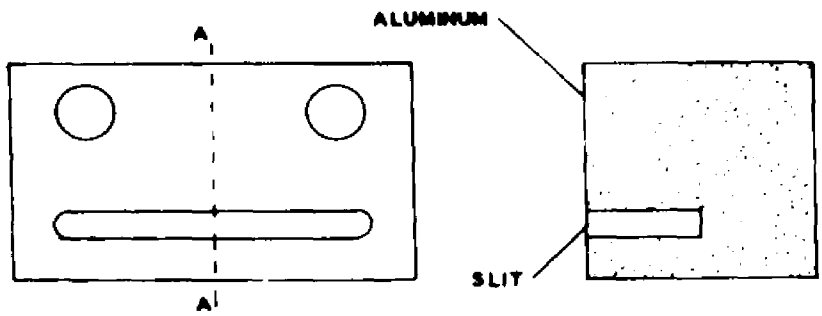

FIGURE 1. SAMPLE HOLDER FOR BOMBARDMENT

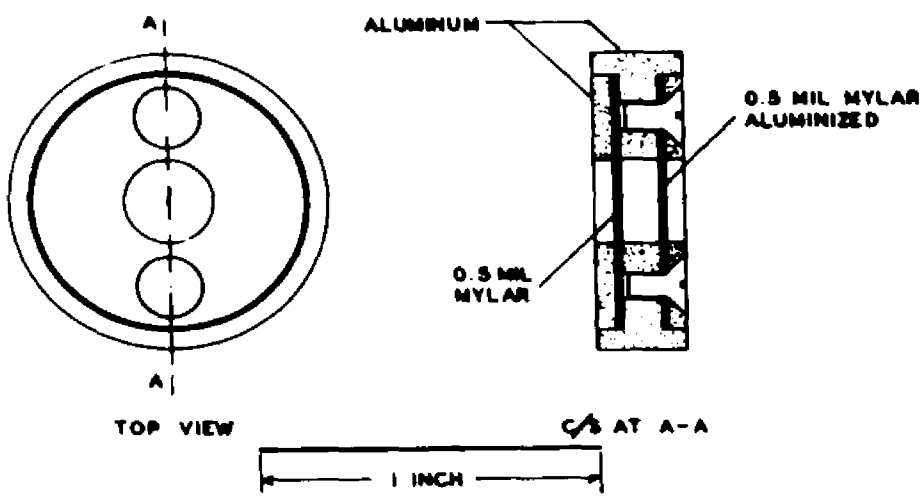

FIGURE 2. GENERAL PURPOSE SAMPLE HOLDER: ALPHA

TABLE 1

ISOTOPIC COMPOSITION OF Gd^{152} AND Sm^{147} SAMPLES

Enriched Isotope	Isotopic Composition		Impurity Content	
	Isotope	Per Cent	Element	Per Cent
Gd-152 (Gd_2O_3)	Gd-152	36.2	Nd	≤0.2
	Gd-154	3.7	Pb,Zr,Pr	0.1
	Gd-155	16.0	Al,Co,Cr,Cu,Mo,Ni,Si,Sn	0.05
	Gd-156	15.6	La,Ce	0.04
	Gd-157	9.2	Ba,Ca,Fe,Mg,Mn,Ti,V	0.02
	Gd-158	11.9	K,Li,Na	0.01
	Gd-160	7.4	Y	0.008
Sm-147 (Sm_2O_3)	Sm-144	0.08	Ca,Pb,Zr	≤0.1
	Sm-147	97.8	Al,Co,Cr,Mo,Ni,Si,Sn	0.05
	Sm-148	0.91	Ba,Cu,Fe,Mg,Mn,Na,Ti,V	0.02
	Sm-149	0.51	K,Li	0.01
	Sm-150	0.17	Be	0.001
	Sm-152	0.34		
	Sm-154	0.21		

Finally the slit was covered with 0.5 mil aluminum foil which was held in place mechanically. The samples were then taken to the Ohio State University Cyclotron where they were bombarded with He^3 nuclei of 16.5 MeV incident energy. The beam was approximately 1 mm in diameter at 1 microampere, and all bombardments had a duration of 60 minutes.

3. SAMPLE PREPARATION FOR SPECTROSCOPY

After bombardment the samples and holders were returned to the Gamma Spectroscopy Lab and portions of the contents remounted in the aluminum sample holders shown in Plate I, Figure 2. (There was one exception to this mounting procedure. A portion of the Sm^{147} sample was placed in a small gelatin capsule, which in turn was sealed in a small glass test tube, for use with a NaI(Tl) well crystal.) The

aluminum holders were designed to hold the radioactive material in good geometry and, at the same time, the thin mylar windows would permit the counting of alpha particles. Flakes of the material selected from the regions of most intense bombardment were carefully placed so that the surface upon which the He^3 nuclei were incident faced up. The sample holders were thereafter handled carefully so that this geometry was not disturbed. Table 2 lists the details of bombardment, the sample number assigned to each isotope, and other pertinent details.

TABLE 2

A LIST OF SAMPLES PREPARED FROM THE He^3 BOMBARDED Gd^{152} AND Sm^{147} ISOTOPES

Enriched Isotope	Sample Number	Mounting Style	Time at End of Bombardment	Duration of Bombardment	Source of Material
Gd-152	N 1827	Alpha	1432 25 May 62	60 min.	New Isotope
Gd-152	N 1840	Alpha	1035 18 Jun 62	60 min.	Reclaimed from Bombardment of 25 May 62
Sm-147	N 1841	Alpha	1145 18 Jun 62	60 min.	New Isotope
Sm-147	N 1842	Well	1145 18 Jun 62	60 min.	New Isotope

4. EXPERIMENTAL APPARATUS

In this investigation multi-channel analyzers were used in conjunction with scintillation detectors and a solid state alpha particle detector for the singles spectra. For the coincidence spectra a transistorized fast-slow circuit was employed. The details of these pieces of apparatus are covered in the following paragraphs.

a. Multi-channel Analyzers

Two multi-channel analyzers were available for use. In general for a particular series of related data the same analyzer was used throughout. The analyzers were a RIDL (Radiation Instrument Development Laboratory, Inc., 4501 West North Avenue, Melrose Park, Illinois) Model 34-12 400 channel transistorized multi-channel analyzer and a RIDL Model 34-12 200 channel analyzer. Each channel of the 400 can store 99,999 counts, while the 200 channel stores 10 times this. The Model 34-12 can analyze up to 10^6 counts per minute and will not distort spectra if operated with less than 5×10^6 counts per minute. The stored information can be presented for visual display or printed out using an IBM electric typewriter.

The basic function of these analyzers is to sort the amplified electrical pulses received from the various detector units according to their amplitude and store them. Thus, one knows both the amplitude of the pulses to an accuracy determined by the channel width and the number of pulses with this amplitude. Since the detectors as well as the electronic circuitry used to amplify the scintillation pulses are linear with respect to energy the channel number is linearly proportional to the energy of the particle or photon producing the pulse in the detector unit. A block diagram of a typical detector-analyzer set up is depicted in Plate II, Figure 3.

b. Coincidence Circuitry

The coincidence measurements were made with a fast-slow system. All the slow circuitry was transistorized. The resolving time of the circuit was of the order of 20 nanoseconds. A block diagram of the

PLATE II
BLOCK DIAGRAMS OF ELECTRONIC APPARATUS

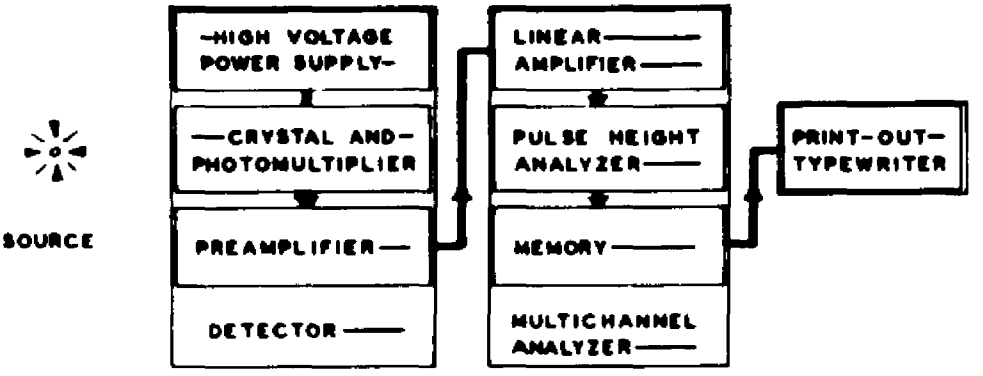

FIGURE 3. TYPICAL DETECTOR-ANALYZER ARRANGEMENT

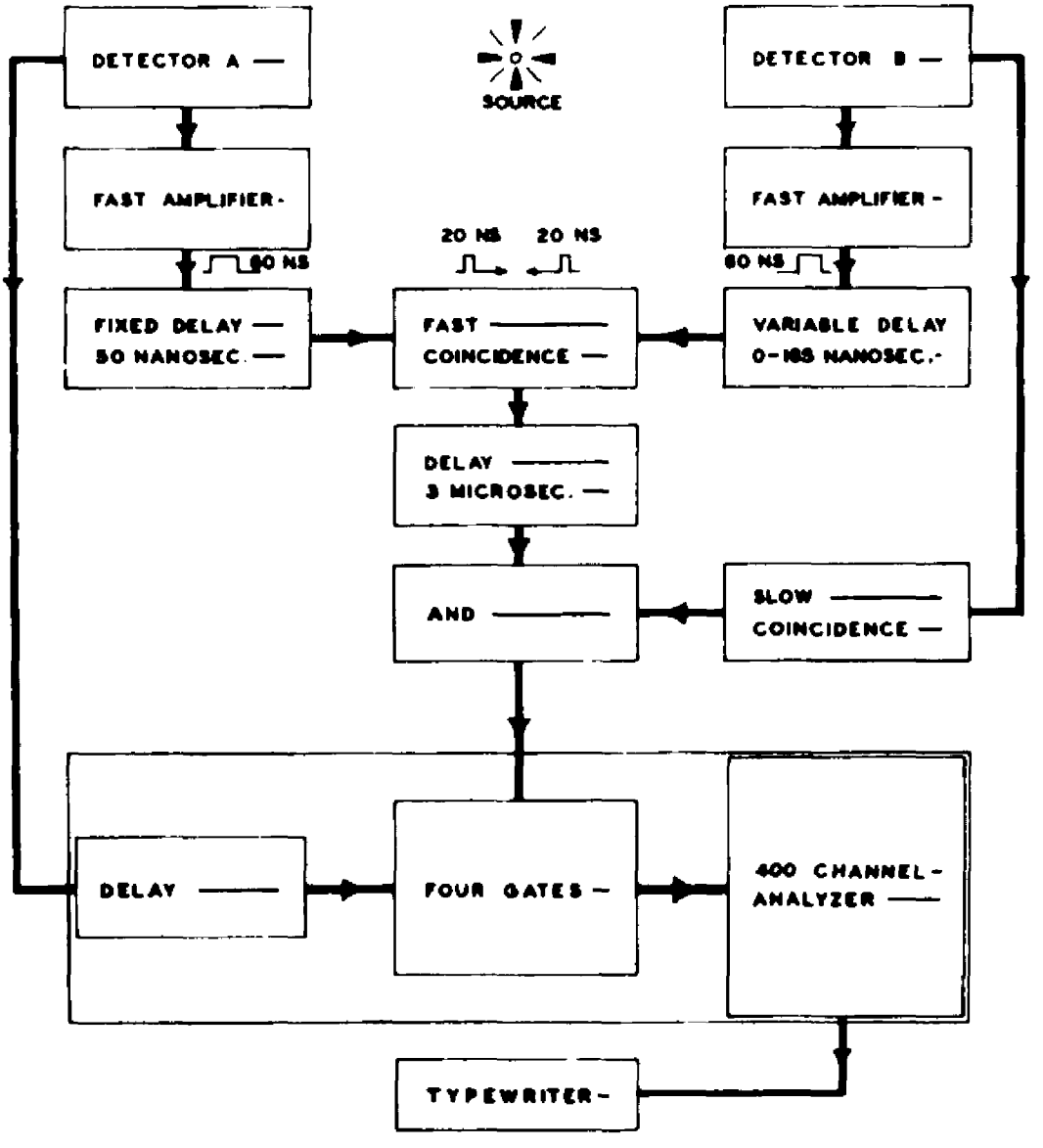

FIGURE 4. FAST-SLOW COINCIDENCE CIRCUIT AND ANALYZER

system is shown in Plate II, Figure 4. With this coincidence arrangement and the 400 channel analyzer it was possible to obtain the singles spectra and coincidence spectra for four different energy intervals during one counting period. The detectors and geometry are discussed under detectors.

c. Detectors

With the exception of the solid state alpha detector, all detectors consisted of a scintillation crystal, a photo-multiplier tube with its associated voltage divider network and a transistorized preamplifier. The specific details of design, geometry, and application are discussed in the ensuing paragraphs.

(1) Cave Crystal (Detector No. 1). The detector employed to obtain decay and unscrambling spectra used a 3"x3" cylindrical NaI(Tl) crystal. The crystal was integrally mounted on a Dumont 6393 photo-multiplier tube and employed a standard RIDL solid state preamplifier. In order to reduce background and scattering this crystal was mounted in a 40"x40"x37" lead cave. The cave was built to specifications given by R. L. Heath[1]. The details of the sample and detector geometry are shown in Plate III, Figure 5. The absorbing material, consisting of aluminum, aluminum oxide, and mylar, between the radioactive source and the crystal was calculated to be 0.14 gm/cm^3.

(2) Well Crystal (Detector No. 2). Summing spectra of the samples was taken with a 3"x3" cylindrical NaI(Tl) well crystal. The packaged (0.032" aluminum) crystal was obtained from the Harshaw Chemical

---

[1]R.L. Heath, Scintillation Spectrometry Gamma-Ray Spectrum Catalogue (TID-4500, Ed 13), p. 13.

PLATE III

DETECTOR SPECIFICATIONS

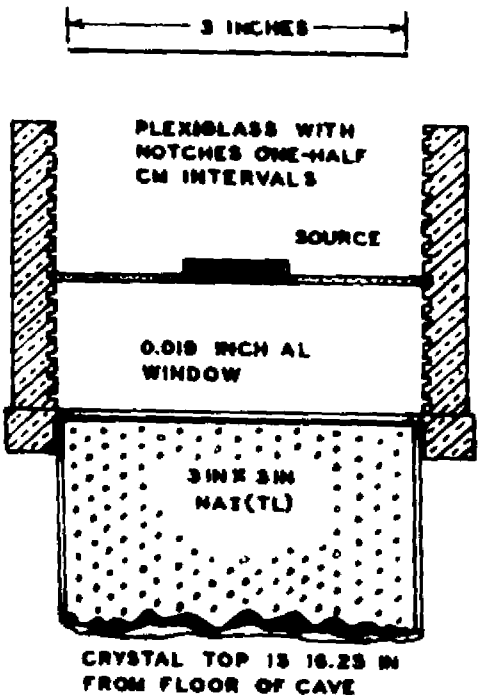

FIGURE 5. GEOMETRY FOR CAVE CRYSTAL

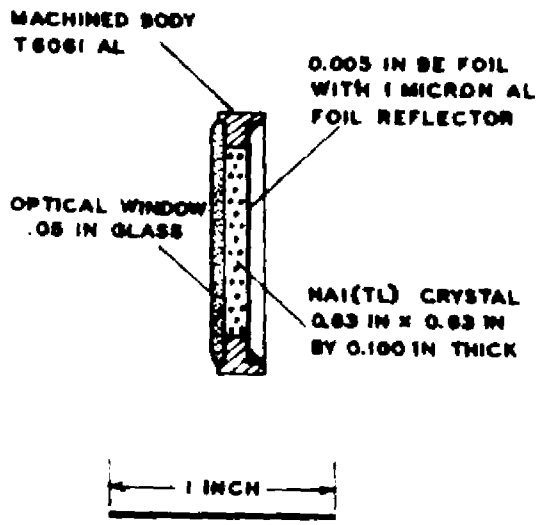

FIGURE 6. X-RAY CRYSTAL

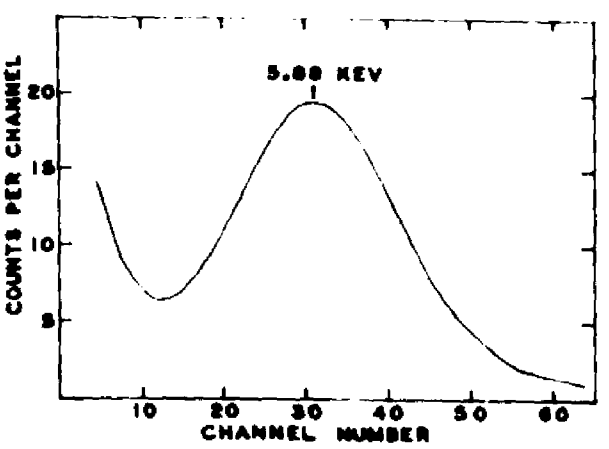

FIGURE 7. X-RAY CRYSTAL RESPONSE TO FE-55 X RAY

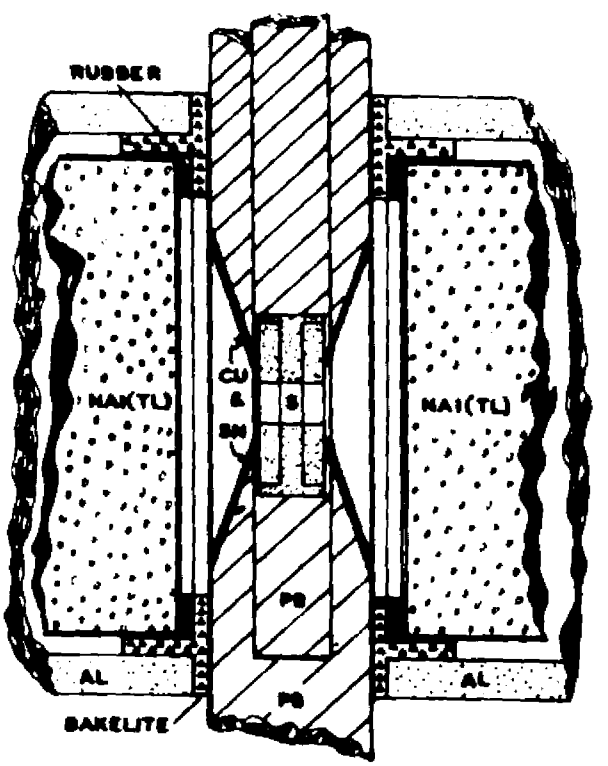

FIGURE 8. COINCIDENCE CRYSTALS GEOMETRY

Company. The specifications of this crystal are given in Plate III, Figure 6. The crystal was mounted on an EMI 6097B photo-multiplier tube. The preamplifier used is transistorized and was especially designed to give high gain with provision for both fast and slow signal output. To obtain high gain the RIDL preamplifier was modified by the addition of two 2N338 transistors. (See Plate IV, Figure 9) The response of the circuit was linear from 5 keV to 100 keV and it exhibited excellent temperature stability. The response of this detector to the Fe^{58} 5.88 keV x ray is shown in Plate III, Figure 7.

The entire assembly was enclosed in a 3" diameter by 9" long aluminum tube and mounted in a vertical position. The sample holder and detector mounting arrangement made it possible to adjust the source to detector distance reproducibly. No shielding was provided for this crystal.

(4) Coincidence Crystals (Detectors No. 7 and No. 8). These detectors, used primarily for coincidence data, employed 1½"x1½" cylindrical NaI(Tl) crystals in conjunction with EMI 6097B photo-multiplier tubes. The preamplifier circuit was the same as that displayed in Plate IV, Figure 8, except for modifications in the values of the resistors R_s, R_1, R_2, R_3, and the dynode at which the slow signal was taken from the photo-multiplier. With these changes the response of the detector was linear up to approximately 2.5 MeV. The housing was similar to that of the x-ray crystal except for the additional length needed to accomodate the larger crystal. The geometry used for coincidence data is shown in Plate III, Figure 8.

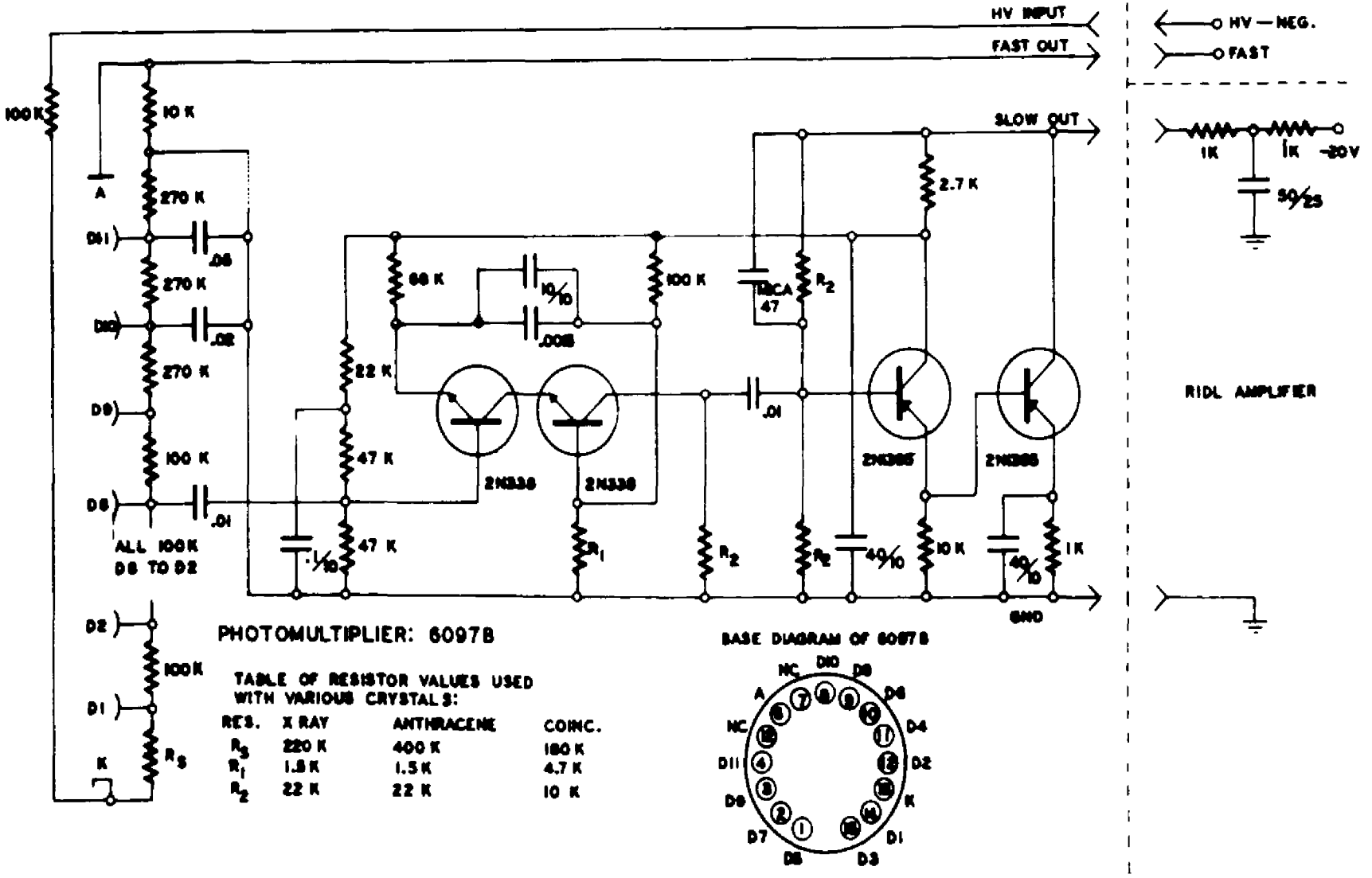

FIGURE 9. EMI 6097B VOLTAGE DIVIDER & PREAMPLIFIER

PLATE IV
FAST-SLOW PREAMPLIFIER

(5) Solid State Alpha Counter (Detector No. 4). A silicon surface barrier detector was used to count alpha particles. The detector and a charge-sensitive preamplifier compatible with the RIDL multi-channel analyzers were obtained from Mr. Denes B. Hunkar, 5914 Cory Avenue, Cincinnati 25, Ohio. The sensitive area of the 7/8" diameter detector was 2.2 cm^2. In the geometry used for counting the solid angle subtended by the sensitive area (with a sample to detector distance of .83 cm) was about 0.4π. The detector and sample were enclosed in an evacuated light-tight aluminum chamber during counting. The sample holders interposed 1.7 mg/cm^2 of mylar (0.5 mil thick) between the radioactive source and the sensitive area of the detector. Two types of chamber were used: one with a thin window of 0.5 mil aluminized mylar under the sample holder so that x rays which were not attenuated significantly could be counted simultaneously with the x-ray crystal without disturbing the geometry; and another with a magnetically operated 0.32 mg/cm^2 aluminum foil shutter which could be interposed between the detector and radioactive source if desired.

The response of the detector to Po^{210} alpha particles is shown in Plate V, Figure 10. Also included on Plate V are curves which show the Po^{210} alpha source with 0.5 mil of mylar (Figure 11) and with 0.5 mil of aluminized mylar (Figure 12) as absorbers. To check the effect of the aluminum shutter a Po^{210} source was prepared in which mylar thicknesses of 0, 0.5, 1.0, and 1.5 mil blocked sections of the source. The results for shutter open are shown in Figure 13 and for shutter closed in Figure 14.

PLATE V

SOLID STATE DETECTOR RESPONSE WITH PO^{210}

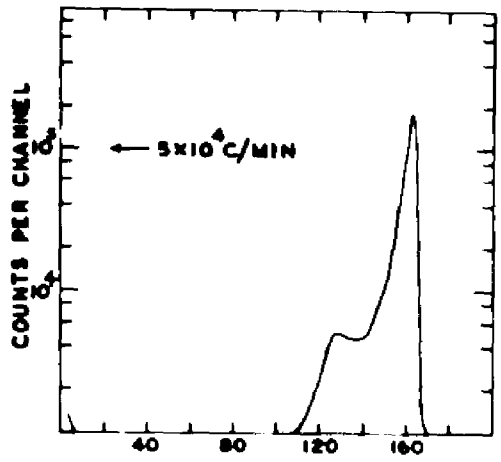

FIGURE 10. PO^{210} & NO ABSORBER

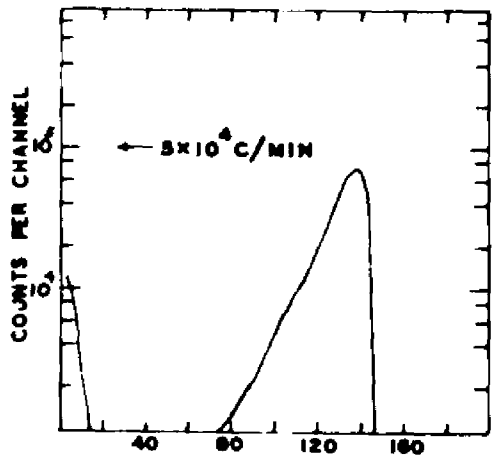

FIGURE 11. PO^{210} & .5 MIL MYLAR

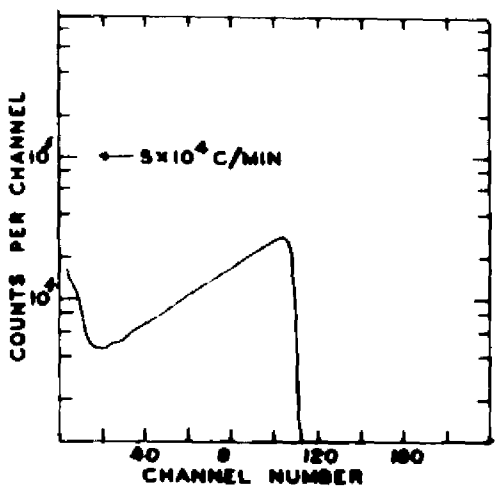

FIGURE 12. PO^{210} & .5 MIL ALUMINIZED MYLAR

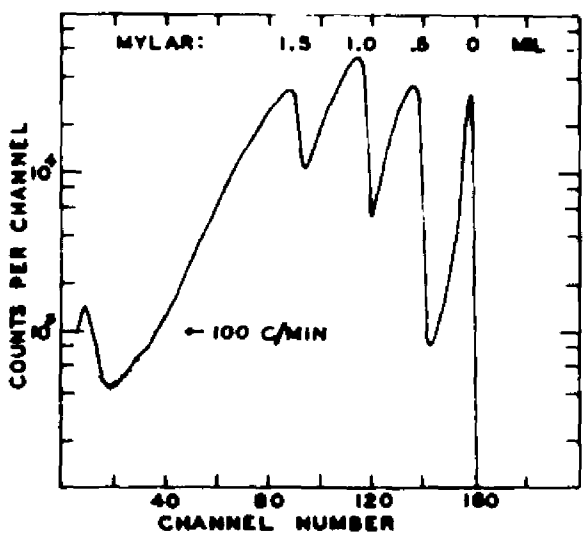

FIGURE 13. PO^{210} WITH GRADED MYLAR ABS. AND .5 MIL AL SHUTTER OPEN

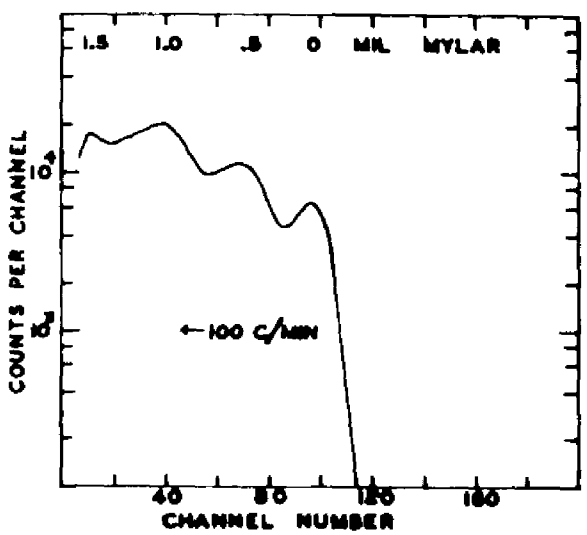

FIGURE 14. PO^{210} WITH GRADED MYLAR ABS. AND .5 MIL AL SHUTTER CLOSED

III. EXPERIMENTAL RESULTS

5. GENERAL COMMENTS

The decay of the activities associated with gamma-rays, x rays, and alpha particles were followed for all Gadolinium and Samarium samples using the cave crystal, the x-ray crystal, and the alpha detector. The energy range examined with photon detectors was from about 20 keV to 2500 keV. All spectra taken were calibrated for energy with known standards, checked for drift during the measurement, and checked for long term (i.e., between spectra) intensity response changes due to equipment or geometry change. The sources used for energy calibrations were Ba^{133}, Cs^{137}, Ce^{144}, Co^{60}, the Gd^{153} x ray ($K\alpha_1$, of Eu^{153}, 41.53 keV), and the Dy^{159} x ray ($K\alpha_1$, of Tb^{159}, 44.47 keV). The latter sources were prepared by proton bombardment of Eu^{153} and Tb^{159} in the Ohio State University Cyclotron. Drift and intensity response of the apparatus were checked by measuring for each spectrum, as appropriate, the response to the 622 keV Cs^{137} gamma-ray, the 1333 keV Co^{60} gamma-ray and the 30.97 keV Ce^{133} x ray produced by the decay of Ba^{133}. The energy range examined with the alpha detector was from about 1 MeV to 6 MeV. The Po^{210} source was used for energy calibration and standardization.

All bombarded samples showed strong activity. The only intense activity observed not associated with either the Samarium or the Gadolinium isotopes was a 511 keV gamma. During the same period the alpha detector spectra showed intense activity from about 1 MeV down

which appeared to be due to beta particles and/or conversion electrons. The half-life of approximately 2 hours associated with the 511 keV gamma was also associated with the high energy beta particle decay observed with the alpha detector. This activity was assigned to oxygen by the reaction: O^{16} (He^3,p) F^{18}, since F^{18} decays by position emission with a half-life of 1.87 hours.

In the following paragraphs the experimental data and the conclusions drawn from these data are discussed. In order to preserve the integrity of the experimental data, the experimental results are presented first and then the interpretations and conclusions are stated.

6. DATA ON GADOLINIUM ACTIVITIES

The principal measurements made on Gadolinium samples, N1827 and N1840, were aimed at identifying the half-lives and the energies of the observed radiations. The cave crystal, coincidence crystals, x-ray crystal and the solid state alpha counter were used to obtain this data.

a. Cave Crystal

With the sample placed 1 cm from the crystal on the crystal axis the spectra of N1827 was followed for 267 days. N1840, prepared from a second bombardment, was used to verify and complete the spectra for the period from 1 to 40 days. The two samples exhibited complete agreement on comparison spectra during this period. Plates VI and VII show six sets of spectra selected from a total of 25 sets as representative of the decay. The energy range covered is from 40 to 2500 keV. The decay half-lives of the gamma rays observed were determined by graphical methods. Table 3 lists in order of decreasing half-life ($T^{1/2}$) the

PLATE VI

GD + HE^3 (GD^{152} ENRICHED) GAMMA RAY SPECTRA

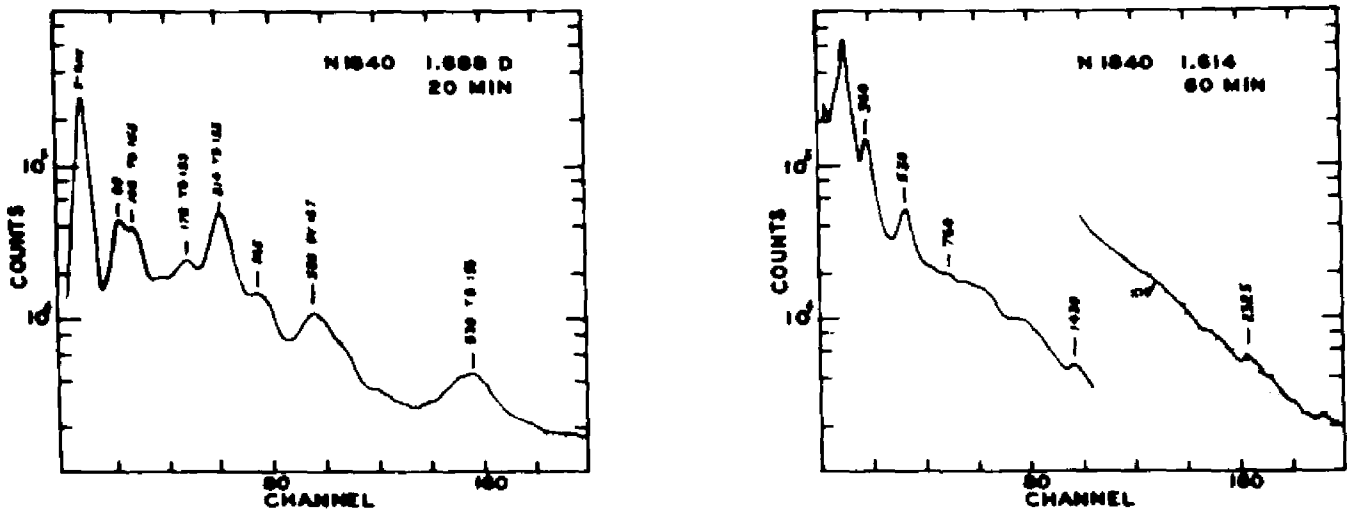

FIGURE 15. SPECTRA AT 2 DAYS

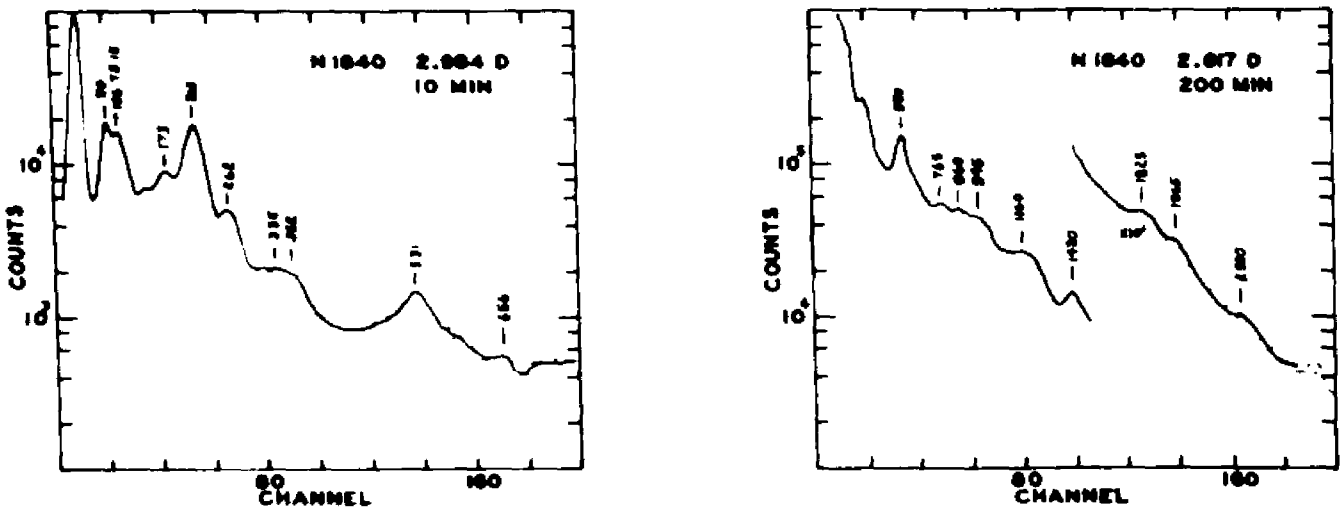

FIGURE 16. SPECTRA AT 3 DAYS

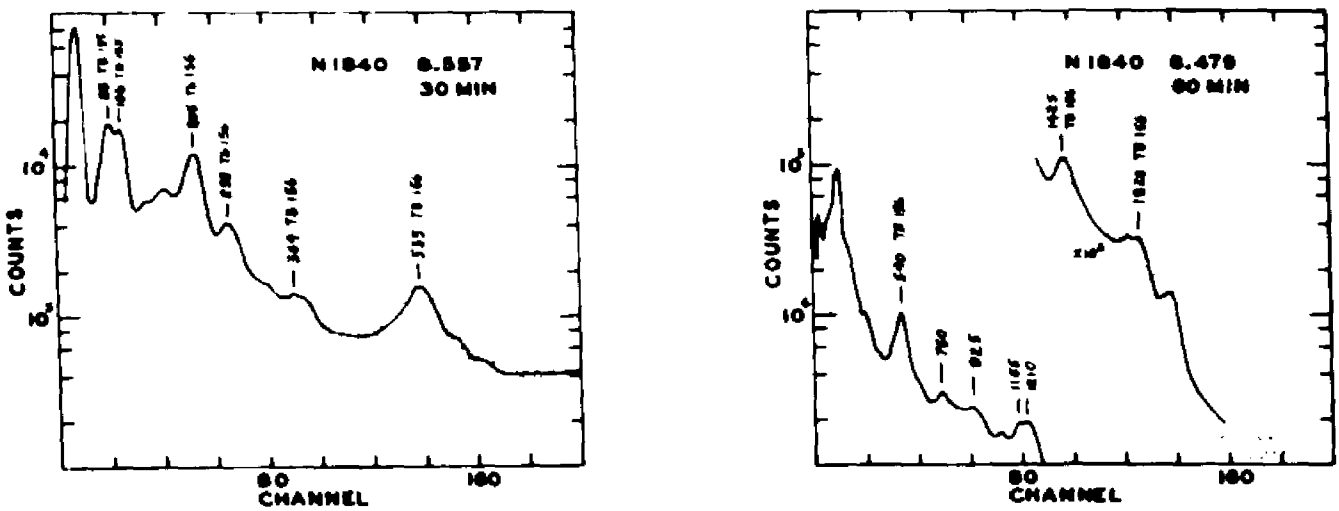

FIGURE 17. SPECTRA AT 9 DAYS

PLATE VII

GD + HE^3 (GD^{152} ENRICHED) GAMMA RAY SPECTRA

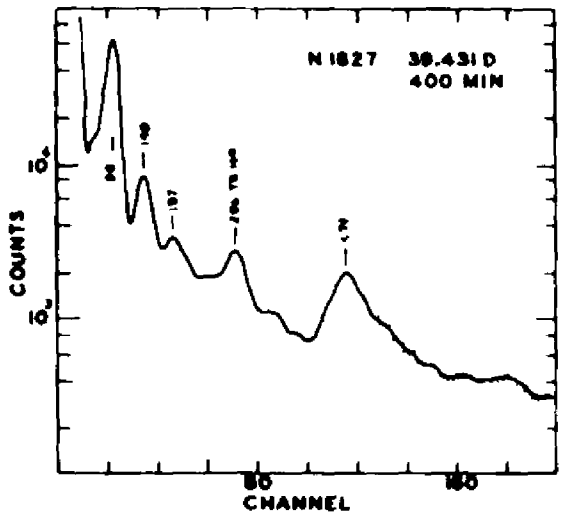

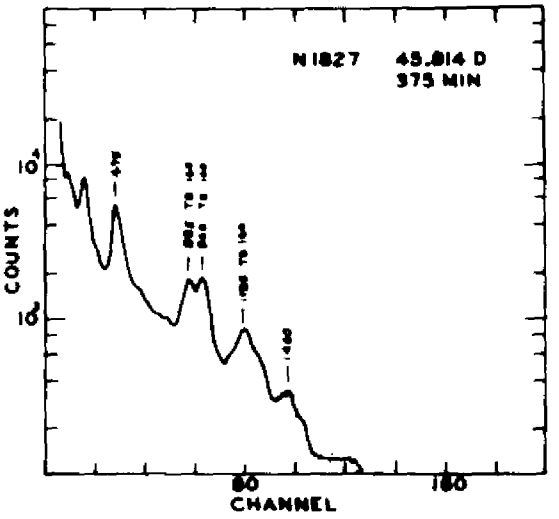

FIGURE 18. SPECTRA AT 40 DAYS

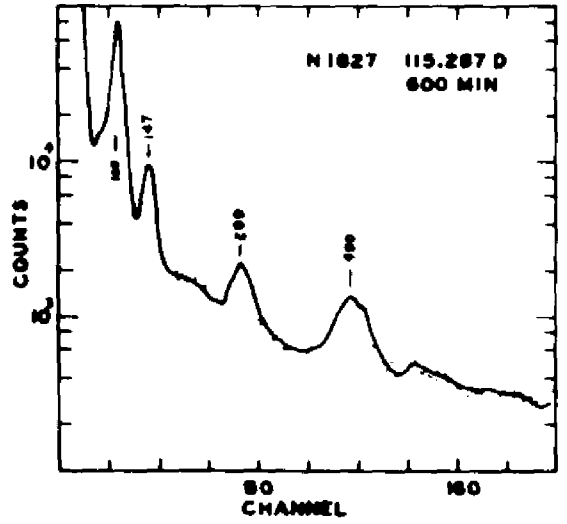

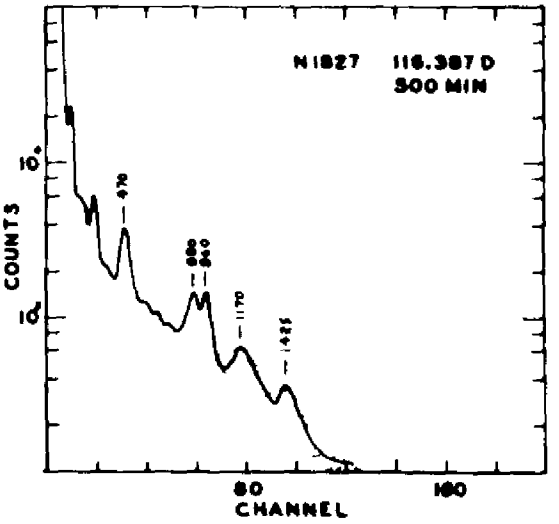

FIGURE 19. SPECTRA AT 120 DAYS

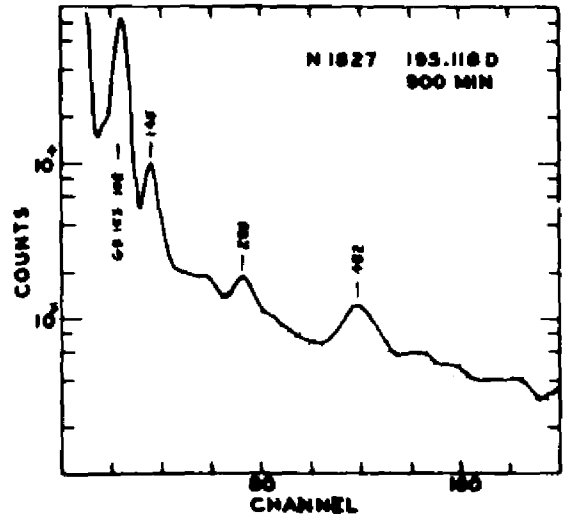

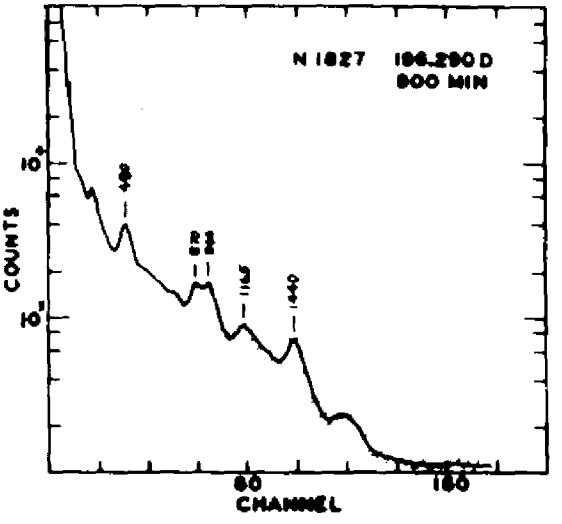

FIGURE 20. SPECTRA AT 200 DAYS

energies of the associated gamma rays. For purposes of reference each gamma ray has also been assigned an identifying number, for example G8 is 1270 keV with a 73 day half-life. The accuracy of the energy assignments for 30 to 600 keV are within ± 5 keV and for 600 keV to 2000 keV within ± 10 keV, while the half-lives are probably within ± 10% of the stated value.

TABLE 3

Gd + He^3(Gd^{152} ENRICHED) GAMMA RAY ENERGIES AND ASSIGNED HALF-LIVES ($T^{1/2}$) OF DECAY

Gamma-Ray Number	Half-life (Days ± 10%)	Energy (keV)	Gamma-Ray Number	Half-life (Days ± 10%)	Energy (keV)
G 1	270	145	G 17	5	760
2	225	101		< 1d	760
3	68	295	18	5	1960
4	60	480*		< 1d	1960
5	73	870	19	< 3	2300
6	73	955	20	< 3	2670
7	73	1170	21	2.3	78
8	73	1270		5.6	78
9	6.0	200		73	78
10	6.0	530	22	2.3	110
11	6.9	354	23	2.3	215
12	5.7	104	24	2.3	254
13	5.6	262	25	2.2	172
14	5.6	172*	26	< 1d	258
15	5.3	1420	27	< 1d	330*
16	5.1	1820	28	< 1d	1080

*Indicates a multiple peak

b. Coincidence Crystals

The only coincidence data obtained was taken at 67 days after bombardment using N1827. Table 4 shows the results of these measurements. The energies indicated are probably accurate to ± 10 keV.

TABLE 4

LOW ENERGY COINCIDENCES IN Gd + He^3(Gd^{152} ENRICHED) AT 67 DAYS

Energy Width of Gate (keV)	Energy of Gamma-Ray (±10 keV) in Coincidence with Gate
20-53	105
62-74	105
83-120	50(1), 120(2), 215(3), 310(3), 415(4), 530(4), 620(4)
129-170	50(2), 80(1), 135(1), 215(1), 300(1), 370(2), 440(2), 520(2), 630(3), 730(3), 810(4), 870(4), 890(4)

() Indicates relative prominence

c. X-ray Detector

The decay of the x ray was followed carefully on both N1827 and N1840. For the decay of N1827, 50 spectra were taken over a period of 268 days. N1840 was observed until it was verified that the samples exhibited no obvious dissimilarities. A total of 28 spectra were obtained over a period of 40 days. In Plate VIII, Figures 21 thru 25 show typical spectra up to 36 days; while Figure 26 shows the energy-time dependence of the x ray. Other than the x ray, the only interesting feature of the spectra is the peak at 31.2 keV which was found to decay with half-life of approximately 2.3 days. Both N1827 and N1840 displayed this peak. The decay of the x ray exhibited half-lives of 230d, 5.3d, 2.4d, 8.5h, and 2.5h as listed in Table 5. The x ray started with the same energy as the Tb $K\alpha_1$ x ray gradually passing through the Gd $K\alpha_1$ x-ray energy at about 3 days and at 256 days was nearly at the Eu $K\alpha_1$ x-ray energy.

GD + HE^3 (GD^{152} ENRICHED) X RAY SPECTRA

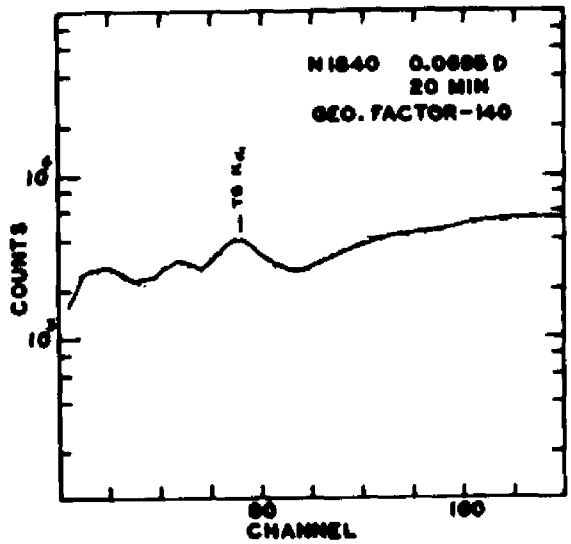

FIGURE 21. SPECTRA AT 2 HOURS

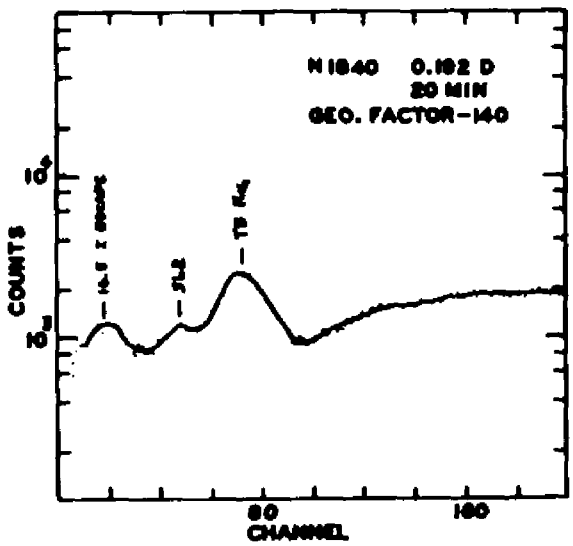

FIGURE 22. SPECTRA AT 5 HOURS

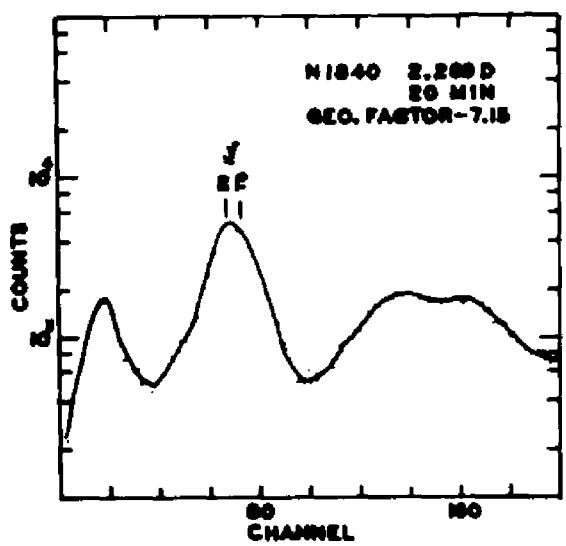

FIGURE 23. SPECTRA AT 2 DAYS

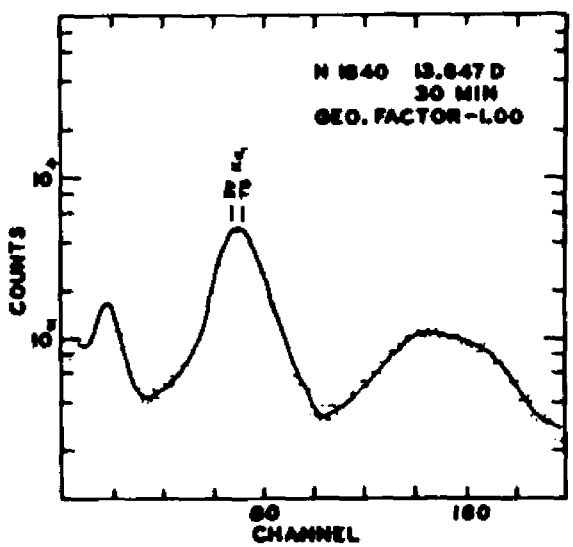

FIGURE 24. SPECTRA AT 14 DAYS

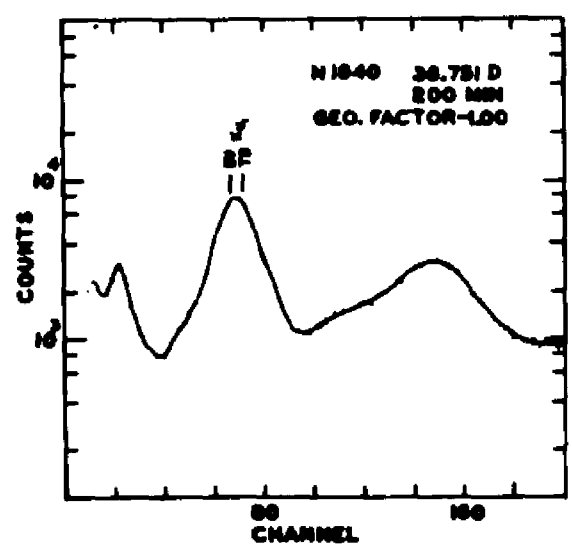

FIGURE 25. SPECTRA AT 37 DAYS

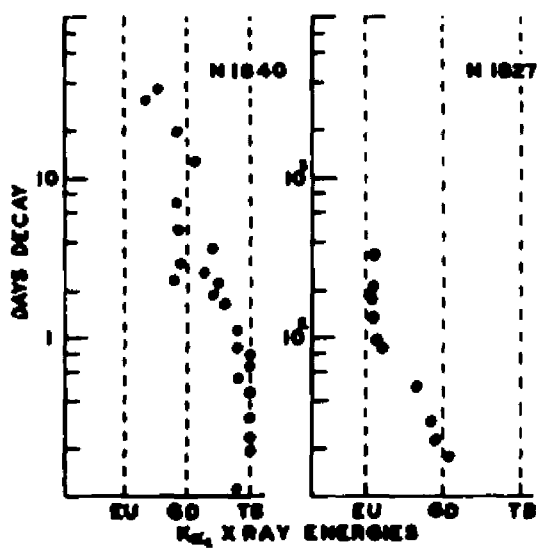

FIGURE 26. ENERGY OF X RAY VS. TIME

Since it was undesirable to move the sample during the early period of decay, and higher energy spectra was needed, additional spectra up to 600 keV were taken with the x-ray crystal on N1827. These low energy gammas were followed for 18 days and, using base lines inferred from cave crystal data, half-lives were able to be associated with the prominent peaks. These are listed in Table 5. Since these peaks were also observed with the cave crystal the x-ray crystal spectra are not presented.

TABLE 5

Gd + He^3(Gd^{152} ENRICHED) GAMMA-RAY ENERGIES AND ASSOCIATED HALF-LIVES OF DECAY (X-RAY CRYSTAL)

Energy (±5 keV)		Associated Half-lives (±10%)
31.2	(G29)	2.3d
x ray		2.5h, 8.5h, 2.4d, 5.3d, 230d
102	(G12)	2.0h, 8h, 2.5d, 5.6d, longer
172	(G14)	1.9h, 9.3h, 2.5d, 5.6d
216	(G23)	1.9h, 9.3h, 2.5d, 5.6d
336	(G27)	1.9h, 8.3h, 5.6d
511		1.9h, 5.5h, 2.6d, 5.5d

d. Alpha-particle Detector

The early spectra taken from N1827 displayed a substantial count rate up to about 1 MeV. This was attributed mainly to pickup of positron and conversion electron induced pulses since the half-lives deduced from the data were not significantly different from those listed in Table 5. As a result no conclusions with regard to alpha activity could be drawn although there appeared to be a higher energy

distribution of pulses above 2 MeV. Table 6 shows a break down of the $T^{1/2}$ associated with a particular energy interval.

TABLE 6

$Gd + He^3(Gd^{152}$ ENRICHED) ACTIVITIES OBSERVED WITH SOLID STATE ALPHA DETECTOR ON M1827

Energy Range (keV)	Associated Half-lives (hours ± 20%)
320-640	15, 2
640-960	20, 2
960-1280	20, 2
1280-2560	20, 2
2560-5120	No significant data

In order to enhance the alpha activity and to reduce the electron contribution the M1840 decay was followed using the aluminum shutter. The shutter was cycled open and closed at regular intervals during a counting period and the difference of the two counting modes taken. These spectra exhibited a sharp fall in count rate up to about 1600 keV followed by an approximately level plateau up to 2800 keV. Thereafter the subtracted spectra fluctuated statistically about zero counts. The decay of the integral count under the plateau is presented in Table 7. Based on the data this activity has a half-life of the order of 5 hours. If account is taken of the mylar window in the sample holder this could be associated with an alpha-particle of about 3.3 ± .3 MeV.

TABLE 7

Gd + He^3(Gd^{152} ENRICHED) DIFFERENCE COUNTS OBSERVED WITH SOLID STATE ALPHA DETECTOR ON M1840

Bombardment Off (Minutes)	Counting Interval (minutes) Clock	Live	Shutter Cycle Time (min)	Shutter Condition	Gross Counts	Net Counts per Min
54	166	100	10	open	532	
				closed	228	6.1±0.6
243	127	100	10	open	367	
				closed	196	3.4±0.5
596	256	240	40	open	595	
				closed	454	1.2±0.3
862	369	360	60	open	948	
				closed	895	0.3±0.1

7. RADIOACTIVE ISOTOPES IDENTIFIED IN GADOLINIUM SAMPLE

Due to the low degree of enrichment of the Gadolinium sample a large number of radioactive isotopes were observed. In order to simplify the comparison of this data with previously reported results Table 8 was prepared. This table lists the isotopic content of the Gadolinium sample, the possible reaction products due to He^3 bombardment and the producing reaction. Many of these isotopes have been investigated by other reaction processes and the results are reported in the literature.[2-25] The half-lives and prominent modes of decay (i.e., gamma-ray and particle energies and intensities) for each isotope which should have been observed in this investigation are

[2] S.K. Bhattacherjee and S. Raman, Nuclear Phys. 1, 486 (1956).
[3] A. Bisi et al., Nuclear Phys. 1, 593 (1956).
[4] B. Harmatz et al., Phys. Rev. 123, 1758 (1961).
[5] K.S. Toth et al., Phys. Rev. 115, 158 (1959).

listed. An abbreviated notation has been used in order to reduce the detail. Thus under Gd^{153} the notation 103(45) G2A means that the 103 keV gamma ray of relative intensity (45) reported for Gd^{153} has been positively identified. The letter A means positive identification and the letter P means possible identification. These facts have been deduced from the data presented in Tables 3 through 7 and Plates VI, VII, and VIII.

As inspection of Table 8 will verify, the presence of Tb^{153}, Tb^{155}, Tb^{156}, Tb^{160}, Dy^{155}, and Dy^{157} is established. The coincidence data supports electron capture of Gd^{153} and beta decay of Tb^{160}. Due to the strong competition of charged particles in the spectra taken with the x-ray crystal and lack of cave crystal data for half-lives

---

[6] K.S. Toth et al., Nuclear Phys. 19, 389 (1960).

[7] R.D. Macfarlane, Natural Alpha Radioactivity in Medium--Heavy Elements (thesis), May 28, 1959. Carnegie Inst. of Tech., Pittsburg.

[8] K.S. Toth and J.O. Rasmussen, Phys. Rev. 109, 121 (1958).

[9] J.O. Rasmussen et al., Phys. Rev. 89, 33 (1953).

[10] R.D. Macfarlane, J. Inorg. & Nuclear Chem. 19, 9 (1961).

[11] K.S. Toth and O.B. Nielsen, Nuclear Phys. 22, 57 (1961).

[12] A.A. Abdurazakov et al., Izvest. Akad. Nauk. USSR, Ser. Fiz. 24, 1126 (1960).

[13] B.N. Subda Rao, Nuclear Phys. 28, 503 (1961).

[14] R.A. Naumann et al., J. Inorg & Nuclear Chem. 16, 163 (1960).

[15] E. Biryukov et al., Izvest. Akad. Nauk. USSR, Ser. Fiz. 25, 109 (1961).

[16] R.C. Greenwood and E. Brannen, Phys. Rev. 120, 1411 (1960).

[17] R.D. Macfarlane and T.P. Kohman, Phys. Rev. 121, 1758 (1961).

[18] 17R.D. Macfarlane and T.P. Kohman, Phys. Rev. 121, 1758 (1961). r Spec18[illegible]

[19] P.G. Hansen et al., Nuclear Phys. 12, 389 (1959).

[20] S. Ofer, Phys. Rev. 115, 412 (1959).

[21] R.E. Bell and M.H. Jørgensen, Nuclear Phys. 12, 413 (1959).

[22] V. Ramsak et al., Nuclear Phys. 6, 451 (1958).

[23] F.D.S. Butement and P. Glentworth, J. Inorg. & Nuclear Chem. 15, 205 (1960).

[24] G.T. Ewan et al., Nuclear Phys. 22, 610 (1961).

[25] S. Ofer, Nuclear Phys. 5, 331 (1957).

TABLE 8

Gd + He^3(Gd^{152} ENRICHED) RADIOACTIVE ISOTOPES OF Dy, Tb, AND Gd

Gd^{152} (36.2%)	Gd^{153}	Gd^{154} (03.7%)	Gd^{155} (16%)	Gd^{156} (15.6%)
10^{14}y α: 2.14	225d E.C. γ': 72(7) 98(51) G2,A 103(45) G2,A	Stable	Stable	Stable
Tb^{152}	Tb^{153}	Tb^{154}	Tb^{155}	Tb^{156}
18.5h(4m) α β+ E.C. γ': 140(3) 235(3) 344(10)G27,P 415(2)	2.6d E.C. γ': 52(10) 68(5) 88(18) G21,A 110(100)G22,A 171(9) G25,A 174(6) G25,A 195(5) 212(120)G23,A 250(6) G24,A	21h(8h) E.C. γ': 88(1) 123(3) 180(5) 250(3) 340(10)G27,P 640(15)	5.6d β+ E.C. 31(?) G29,A 60(4) 87(50)G21,P 105(35)G12,A 149(4) 163(12)G14,A 182(11)G14,A	5.4d(5h) E.C. γ': 89(9) G21,P 200(5) G 9,A 260(1) G13,A 355(2) G11,A 535(8) G10,A 1045(1) 1140(2) 1400(2) 1815(.4)G16,A
Dy^{152}	Dy^{153}	Dy^{154}	Dy^{155}	Dy^{156}
2.5h α: 3.7 E.C.	5h α: 3.5 β+	13h α: 3.35 or 10^6y α: 2.85	10h E.C. γ': 65(33) 91(6) G21,A 227(100)G23,A 660(7) 880(3)	Stable

TABLE 8 (Contd.)

Gd^{157} (9.2%) Stable	Gd^{158} (11.9%) Stable	Gd^{159} 18h β^-: 950(76) 600(16) 890(8) γ': 57(26) 364(9)	Gd^{160} (7.4%) Stable	Gd^{161} 3.6m β^-: 1600 γ': 36 102
Tb^{157} > 30y E.C.	Tb^{158} > 3y E.C.	Tb^{159} Stable	Tb^{160} 73d β^- γ': 87(68)G21,A 298(28)G 3,A 871(34)G 5,A 964(25)G 6,A 1175(16)G 7,A 1272(8) G 8,A	Tb^{161} 7d β^- γ': 26(8) 49(8) 57(3) 75(1)
Dy^{157} 8.2h E.C. γ': 61(6) 83(24) G21,A 182(9) 265(4) G26,P 327(990)G27,A	Dy^{158} Stable	Dy^{159} 144d E.C. γ': 58(3)	Dy^{160} Stable	Dy^{161} Stable

less than 1 day no positive conclusions can be drawn about the exact energies. The half-lives obtained with the x-ray data do make highly probable the presence of Dy^{152}. The 511 annhilation radiation and the results from the alpha-particle detector indicate the presence of Dy^{153}. In the case of Dy^{154} no conclusive statement can be made. Quite possibly the 13 hour alpha decay reported by Toth[8] could have been missed but the absence of gamma radiation with this half-life tends to support the 2×10^6 year alpha decay reported by Macfarlane[10].

Several gamma rays were observed which are not accounted for in the literature. These are G1 (145 keV, 270 days), G17 (760 keV, 1d and 25d), G18 (1960 keV, 1d, and 5d) and G19 (2300 keV, 3d). The short half-life gamma rays G17, G18, and G19 cannot be assigned on the basis of this data. Nevertheless their presence indicates that further detailed investigation of the early decay of samples with this enrichment of Gd^{152} can be of significant value. G1 cannot be associated with any isotope or impurity on the basis of previously reported data. The complex results of the coincidence data cannot be explained by the presence of Gd^{153} and Tb^{160} alone. The coincidence data shows a very complex structure associated with G1. In addition there appear to be peaks at $\sim$ 230, 295 and $\sim$ 350 decaying with the same half-life (see Plate VII, 200d). This data is insufficient to make it possible to draw definite conclusions, but if the isotopic abundances are considered and we note the quantity of Tb^{160} produced, it is highly reasonable to assume that an appreciable amount of Tb^{158} was also

---

[8] Toth, op. cit., p. 121.
[10] Macfarlane, op. cit., p. 9.

produced. The predominant mode of beta decay for Tb^{158} would explain the low intensity of the x ray associated with this line in the coincidence data. Tb^{157} is also a possibility that cannot be eliminated except that it has to decay by electron-capture and this is at variance with the coincidence results. These conclusions are not in agreement with those of Butement and Glentworth[23] who identified Tb^{158} from a spallation reaction as decaying by K capture with a half-life of > 3 years.

8. DATA ON SAMARIUM ACTIVITIES

Essentially the same procedure in taking data was employed on the Samarium samples as with the Gadolinium samples. Energies of prominent gamma rays and half-lives were followed with the cave crystal. The decay and energy of the x ray were observed with the x-ray crystal. In addition, since the spectra was not as complex due to the high enrichment of Sm^{147}, well data and coincidence data were useful for identifying isotopes; while the unscrambling spectra, used in conjunction with information obtained from the literature, made it possible to determine the relative amounts of each radioactive isotope produced in the bombardment. This data and the analysis of the data are presented in the following paragraphs.

a. Cave Crystal

The spectra from N1841 was followed from 1 day to 350 days on the 3"x3" NaI(Tl) crystal. A total of 18 spectra for each energy range

---

[23]Butement and Glentworth, op. cit., p. 205.

(50 keV to 700 keV and 300 keV to 2250 keV) were taken. The sample geometry was as shown in Plate III, Figure 5, with a source to crystal distance of 1 cm. The results of these measurements are shown in Table 9. The methods used in obtaining energies and half-lives have been described previously. The accuracy of the assignments is the same as that given for the Gadolinium samples. Plates IX and X show the spectra at various periods of the decay. In order to obtain a better estimate on the half-lives of decay in the high energy spectra integral counts from 135 keV to 2460 keV were plotted versus time after bombardment. Two half-lives predominated, 55.9 and 26.4 days, with the shorter half-lives undetermined; while the longer half-lives did not contribute significantly to the integral count in this energy range.

b. Well Crystal

The sum spectra were obtained from N1842 at 2 days and 163 days in the decay of the Samarium sample. A summary of the results is listed in Table 10, while Plate XI shows the "in-well", "out-well", and difference spectra.

PLATE IX

$SM+HE^3$ (SM^{147} ENRICHED) GAMMA RAY SPECTRA

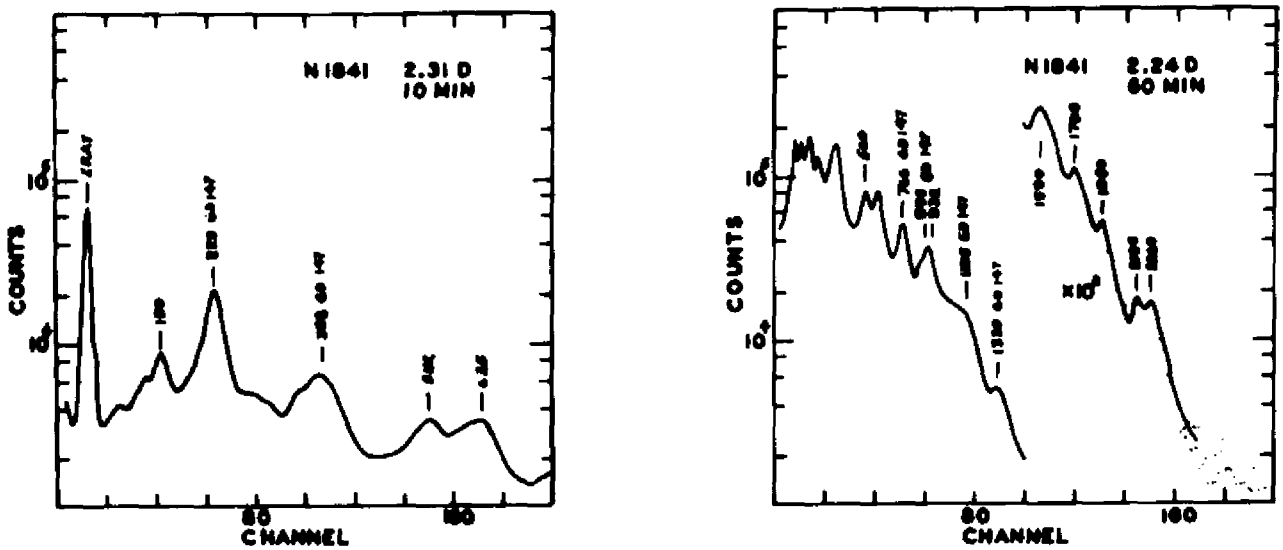

FIGURE 27. SPECTRA AT 2 DAYS

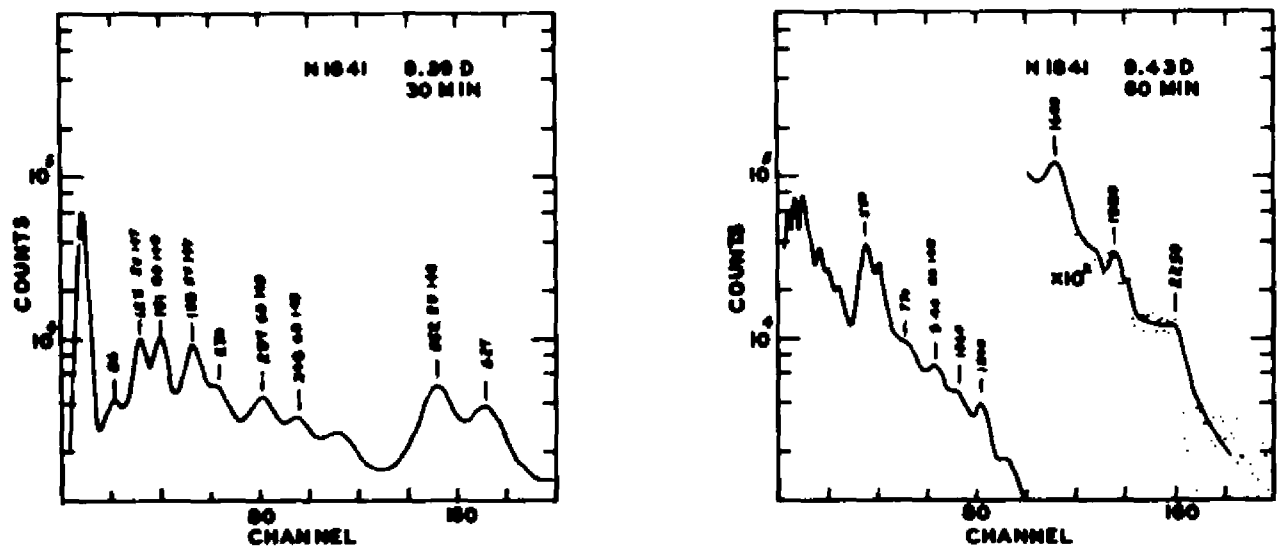

FIGURE 28. SPECTRA AT 8 DAYS

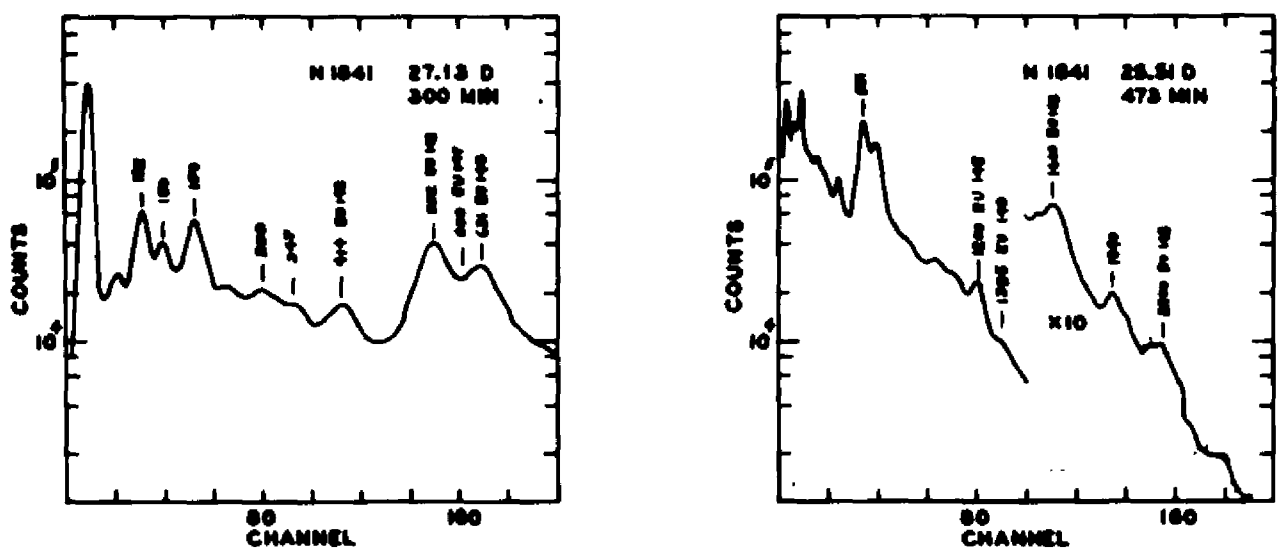

FIGURE 29. SPECTRA AT 26 DAYS

PLATE X

SM+HE^3 (SM^{147} ENRICHED) GAMMA RAY SPECTRA

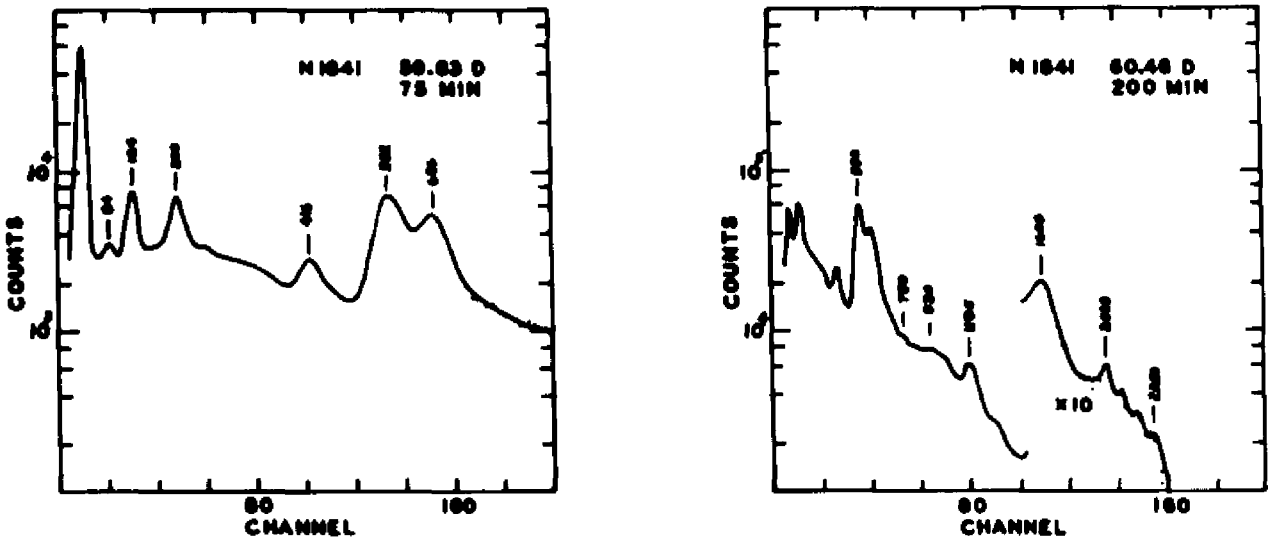

FIGURE 30. SPECTRA AT 80 DAYS

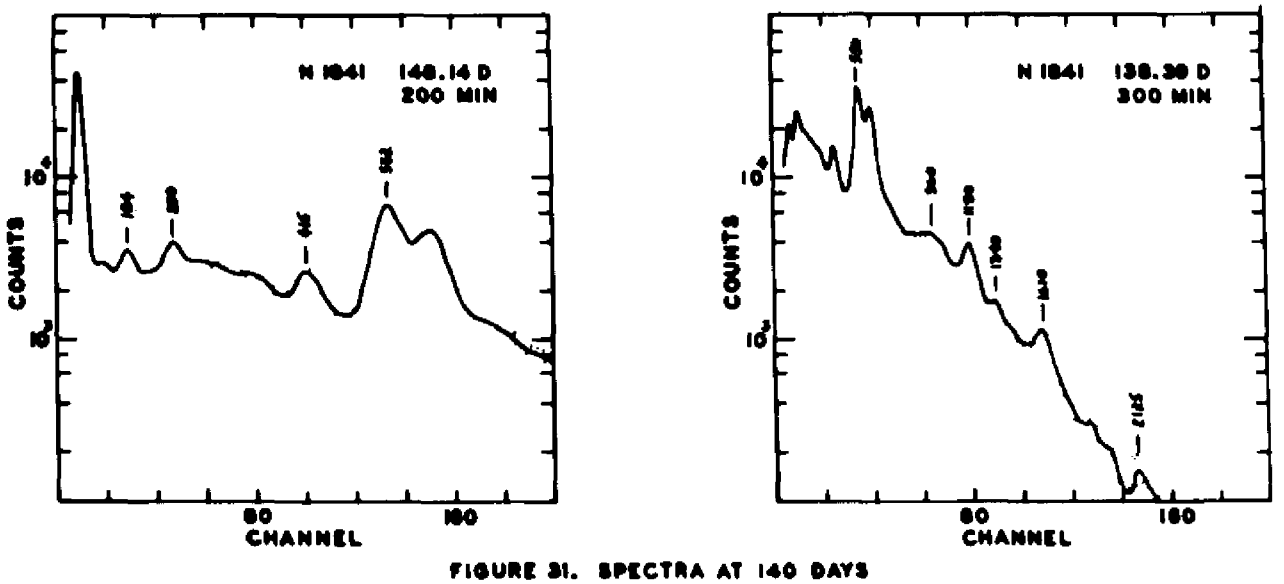

FIGURE 31. SPECTRA AT 140 DAYS

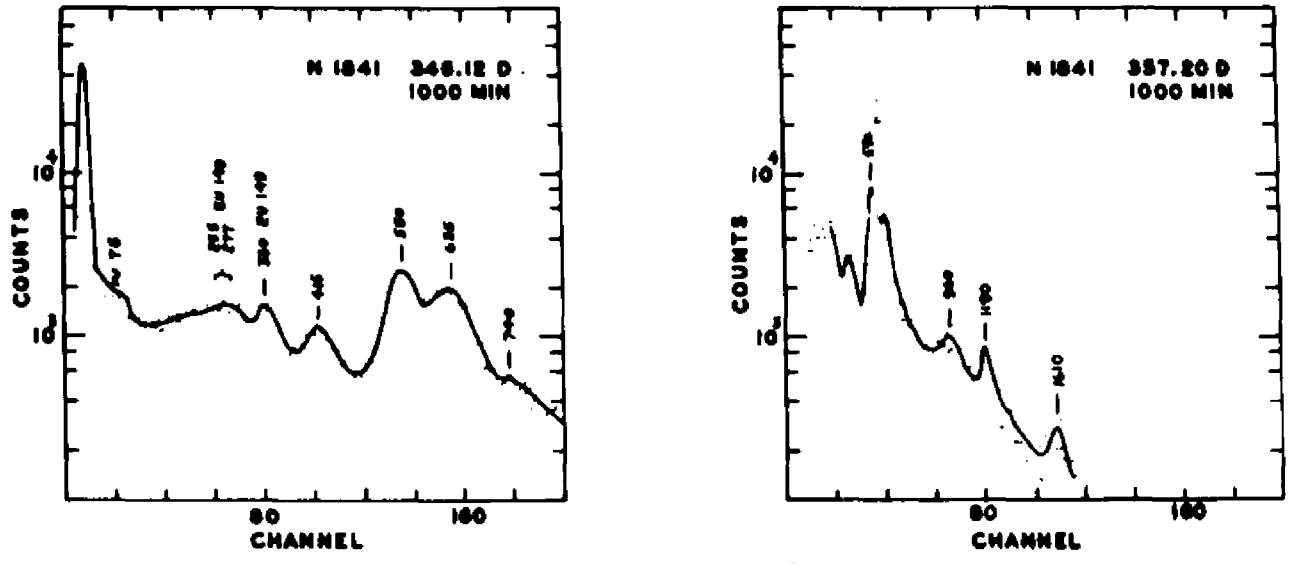

FIGURE 32. SPECTRA AT 350 DAYS

TABLE 9

Sm + He^3(Sm^{147} ENRICHED) GAMMA-RAY ENERGIES AND ASSIGNED HALF-LIVES (CAVE CRYSTAL)

Gamma-Ray Number	Half-life (days ± 10%)	Energy (keV)	Gamma-Ray Number	Half-life (days ± 10%)	Energy (keV)
S 1	103	58?	S26	25	630
S 2	103	78?	S27	22	198
S 3	90	267*	S28	22	123
S 4	70	328	S29	10	150
S 5	70	342	S31	8	342
S 6	60	2180	S32	8	300
S 7	58	1040*	S33	<2	1790
S 8	58	945*	S34	<2	890
S 9	58	800	S35	<2	770
S10	58	630	S36	<2	630
S11	58	415	S37	<2	229
S12	58	200	S38	<2	370
S13	58	80	S39	<2	396
S14	56	865	S40	<2	560
S15	55	2060	S41	<2	932
S17	55	1600*	S42	<2	260
S18	55	1510	S43	<2	1130
S19	55	1185	S44	<2	1330
S20	55	1330	S45	<2	1590
S21	55	553	S46	<2	1790
S22	54	712*?	S47	<2	1960
S23	28	1060*	S48	<2	2180
S24	25	945*	S49	<2	2260
S25	25	800			

* A multiple peak
? Uncertain peak

PLATE XI

$SM+HE^3$ (SM^{147} ENRICHED) SUM SPECTRA

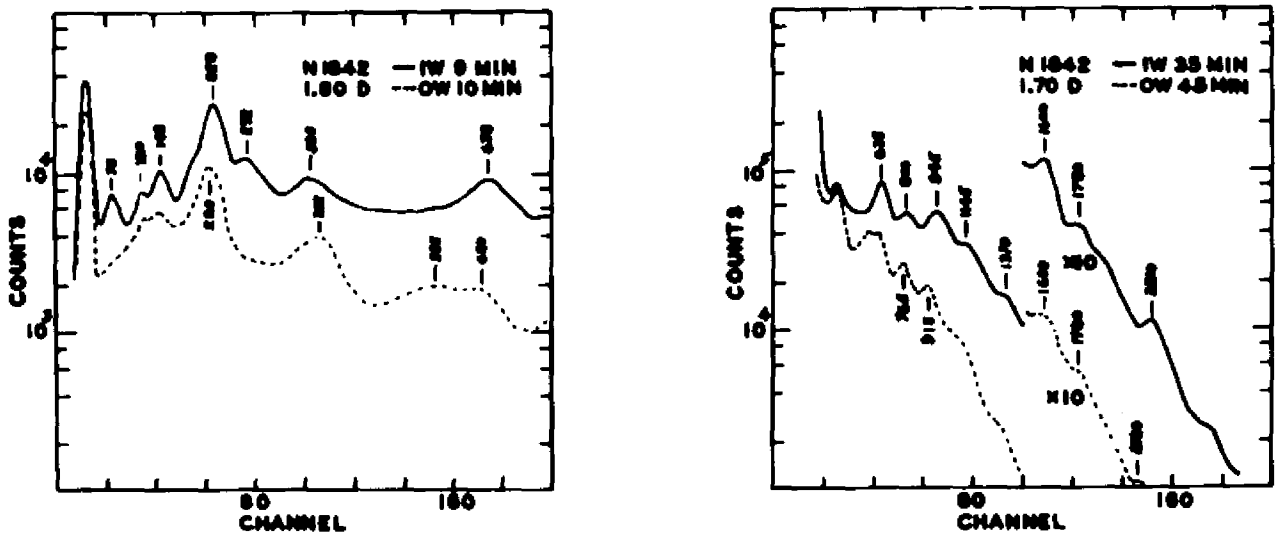

FIGURE 33. SUM SPECTRA: IN WELL & OUT WELL AT 2 DAYS

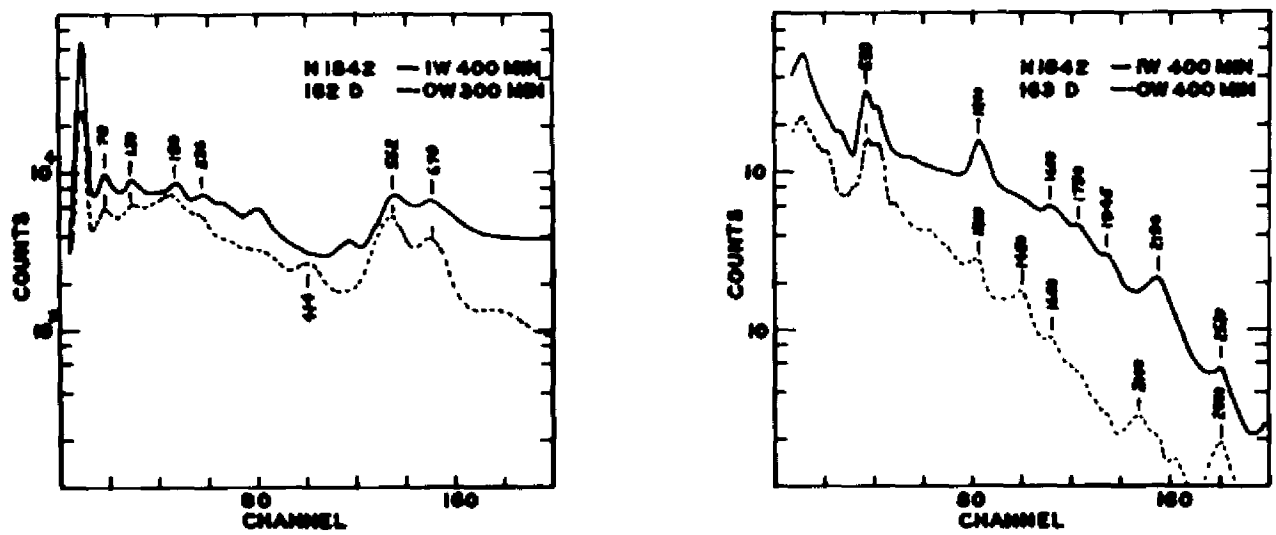

FIGURE 34. SUM SPECTRA: IN WELL & OUT WELL AT 160 DAYS

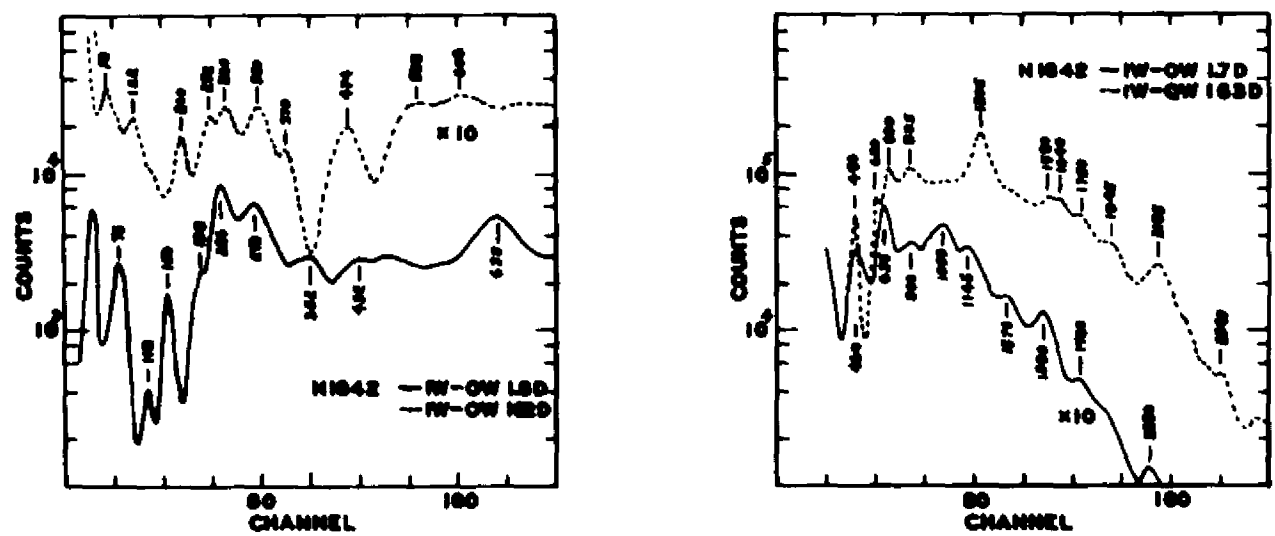

FIGURE 35. IN WELL-OUT WELL AT 2 AND 160 DAYS

TABLE 10

Sm + He^3(Sm^{147} ENRICHED) SUM PEAK ENERGIES OBSERVED WITH WELL CRYSTAL

Days After Bombardment	Sum Peak Energies Observed (keV)
1.693	330, 450-485, 530, 635, 675?, 765-825, 890-1000, 1145, 1230?, 1370, 1425?, 1580, 1630?, 1785, 1920, 2180, 2430?, 2550, 2620?. (all ± 15 keV)
1.784	76, 118, 150, 197, 226, 270-275, 330-352, 378?, 402?, 432?, 464-484, 512?, 548-562, 606?, 638, 670?. (all ± 5 keV)
162.17	78, 100?, 122, 154, 200, 252, 274-282, 330, 370, 474, 530?, 560?, 588, 620, 638, 668, 690. (all ± 5 keV)
163.15	487, 620, 690, 784-825, 990-1040, 1200, 1380, 1450, 1515, 1580-1640, 1750, 1800, 1890-1940, 2000, 2200, 2340, 2450, 2540. (all ± 15 keV)

? Uncertain

c. Coincidence Crystals

Coincidence data was taken on N1841 at 18 days and 30 days. A highly complex structure was obtained at 18 days as can be seen from Table 11. In this table the energies of the gamma rays are listed as well as the number inclosed in parenthesis which indicates the relative prominence of the particular gamma ray. An estimate of the average spectral intensity is also included for purposes of comparing the spectra qualitatively. The 30-day data concentrates principally on low energy gamma rays and is presented in Plate XII. These spectral

TABLE 11

Sm + He^3(Sm^{147} ENRICHED) COINCIDENCE SPECTRA AT 19 DAYS

Count Time	Spectral Intensity (cts/min)	Coinc. Gate (keV)	Coincidence Gammas & Relative Prominence
300 min at 18.3d	0.23	362-384	x ray(5),123(2),150(2),315(4),415(4),554(1),620(4).
	0.23	414-430	x ray(4),123(3),150(3),210*(2),260(3),300(3),400(4),550(1),620(3).
	1.00	510-562	x ray(5),200(2),245(3),300(4),415*(2),550*(2),620(1).
	0.50	600-634	x ray(7),85(5),125*(3),210*(3),240(4)415(4),450(6),550(1),620(6).
400 min at 18.6d	0.43	222-256	x ray(3),100(4),123(2),150(2),204(2),250(3),315(3),415(3),430(4),480(5),545(1),620(4).
	0.33	270-292	x ray(4),80(5),123(4),150(2),200(3),400(4),415(3),555*(1),620(4),710(6).
	0.43	332-366	x ray(7),100(4),117(7),158(1),188(3),310(6),340(6),420(4),446(5),555(2),620(4),
	0.55	380-420	x ray(5),130(3),208(2),310(3),340(3),400(4),550(1),620(3).
400 min at 19.0d	0.03	70-94	x ray(6),90(4),121(1),158(2),206(2),240(3),410(4),550(5).
	0.09	112-132	x ray(4),100(4),134(1),158(2),206(2),245(3),350(4),390(5),430(7),572(5),654(5).
	0.15	142-158	x ray(3),100(3),135(2),150(2),206(2),232(2),347(1),428(3),552(3),632(4),695(5).
	0.32	184-210	x ray(1),114(1),150(1),206(1),308(3),420(3),552(2),620(4).
550 min at 19.5d	0.55	535-680	200(1),410(2),545(1),620(3),720(4),900(5),1010(6),1170(7),1340(7),1480(9),1650(8).
	0.05	790-910	200(1),410(2),545(1),620(3),780(4),900(4),1010(5),1970(5),1130(6),1240(6),1340(6),1670(6).
	0.04	1010-1190	410(2),545(1),620(2),720(3),900(4),1010(5),1220(6),1340(7),1480(8),1670(8).
	0.03	1260-1430	200(2),340(3),545(1),620(2),780(4),900(4),1070(5),1280(5).

* Multiple peak

distributions have the same shape but are less complex than the more complete data taken at 18 days.

d. X-Ray Crystal

A total of 20 spectra were taken from N1841 in following the decay of the x ray for 350 days. Representative spectra and the energy-time dependence of the x ray are shown in Plate XIII. The x ray started at the Europium $K\alpha_1$ x-ray energy and by 20 days was at the Samarium $K\alpha_1$ x-ray energy. It remained there when the last data was taken. The associated half-lives were found to be $\sim$103, 54, 25, 9 and 1 day.

e. Solid State Alpha Detector

Using the 0.5 mil aluminum shutter the counts obtained from N1841 in the energy range of 1000-2200 keV for the period 6.95 to 13.95 hours after bombardment was 102 ± 56 counts (0.43 counts/minute) and for the period 154.75 to 174.75 hours after bombardment was 154 ± 86 counts(0.26 counts/minute). The spectra showed a plateau like distribution terminating at 2000 keV. Thus these counts could result from an alpha particle of approximately 3 MeV energy. If a single alpha was involved in the decay the associated half-life lies in the neighborhood of 7 days.

f. Unscrambling Spectra

Cave crystal spectra was taken on N1841 8 days after bombardment. The geometry has been described. In order to reduce the sum peak contributions, the source was placed 5 cm from the crystal. At this distance the sum peak of Co^{60} had approximately one-fiftieth of the number of counts in the 1330 keV peak. Plate XIV shows the three sets

PLATE XII

$SM + HE^3$ (SM^{147} ENRICHED) COINCIDENCE SPECTRA

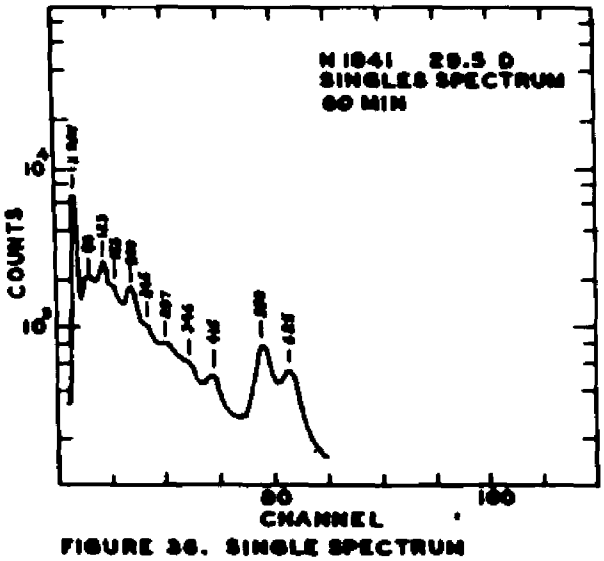

FIGURE 36. SINGLE SPECTRUM

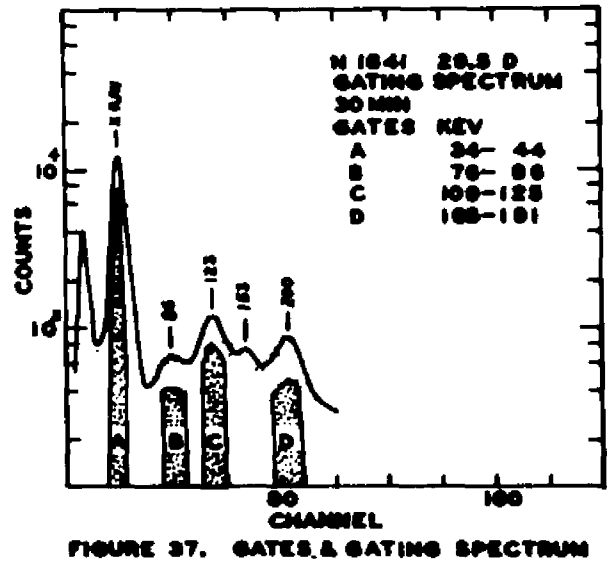

FIGURE 37. GATES & GATING SPECTRUM

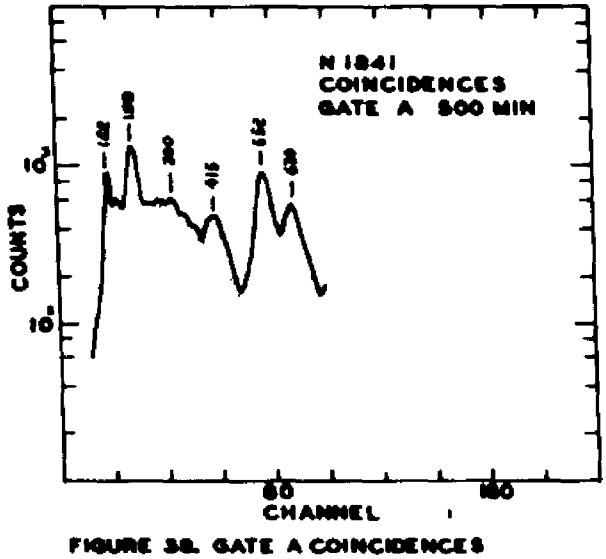

FIGURE 38. GATE A COINCIDENCES

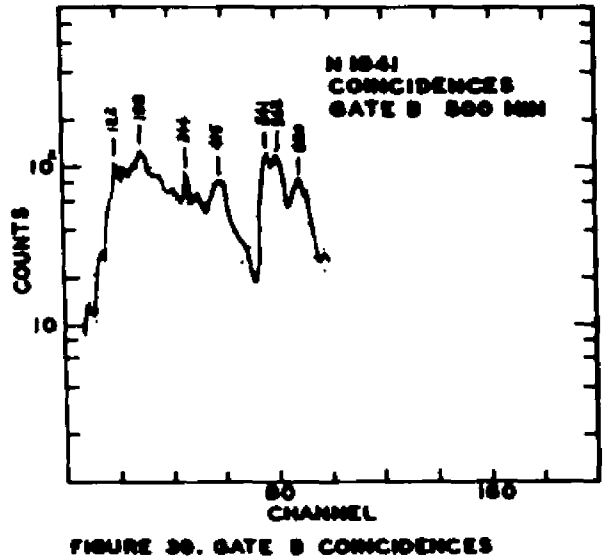

FIGURE 39. GATE B COINCIDENCES

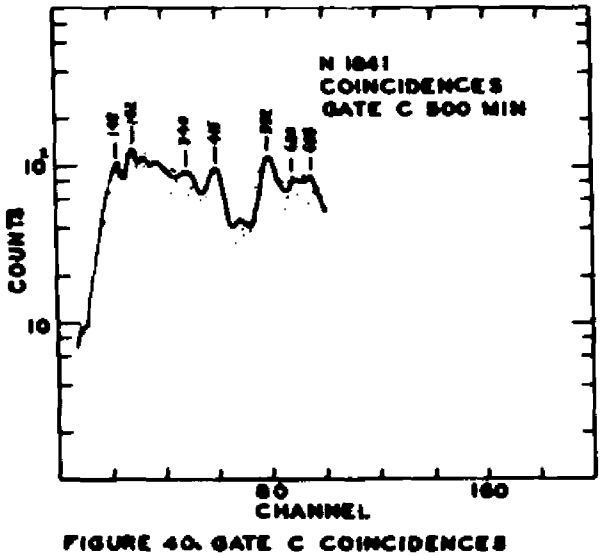

FIGURE 40. GATE C COINCIDENCES

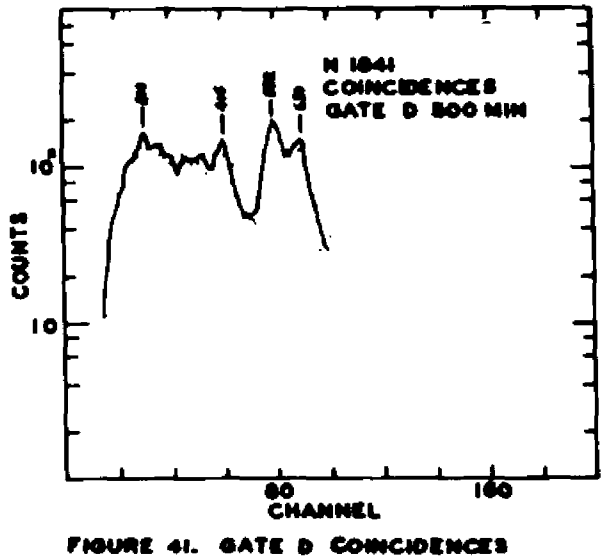

FIGURE 41. GATE D COINCIDENCES

PLATE XIII

$SM + HE^3$ (SM^{147} ENRICHED) X RAY SPECTRA

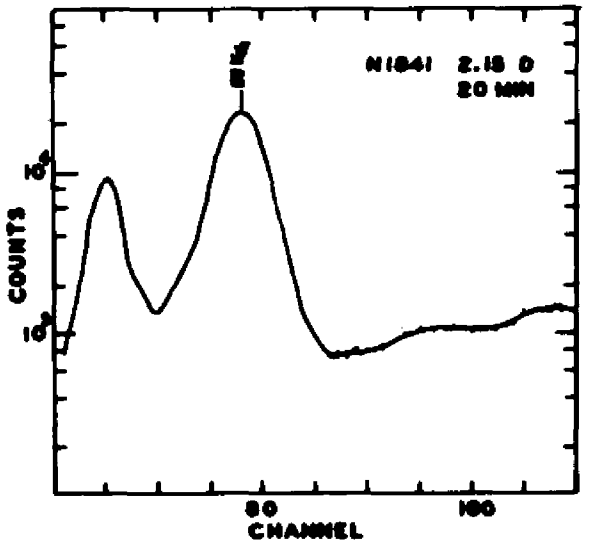

FIGURE 42. SPECTRA AT 2 DAYS

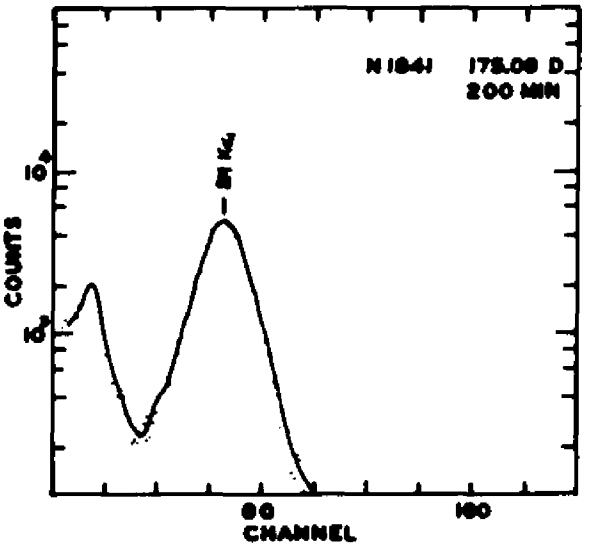

FIGURE 43. SPECTRA AT 175 DAYS

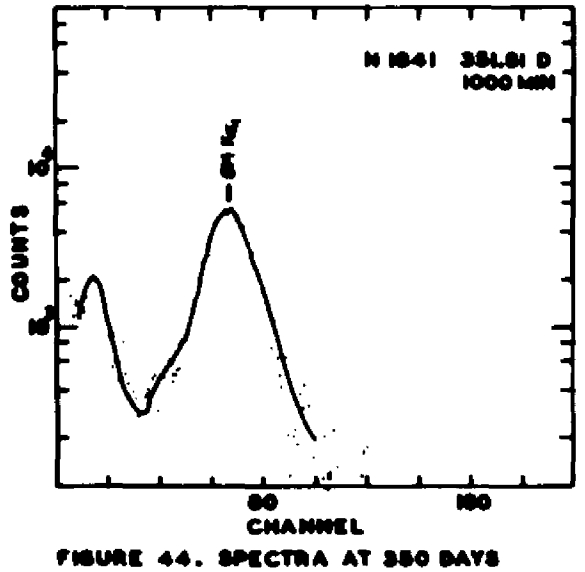

FIGURE 44. SPECTRA AT 350 DAYS

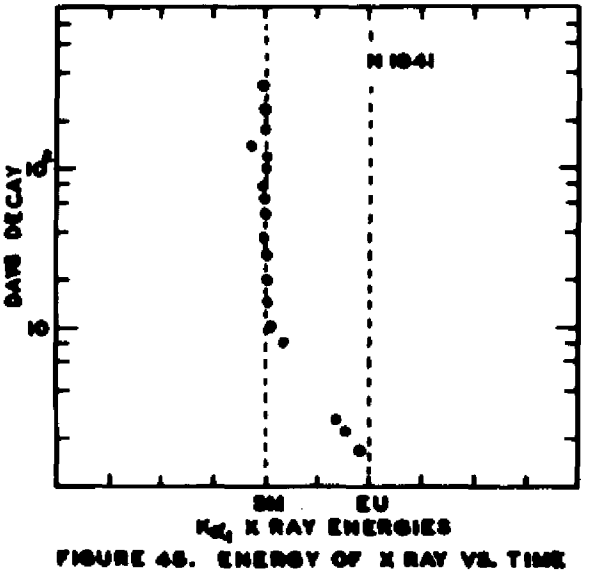

FIGURE 45. ENERGY OF X RAY VS. TIME

of spectra which were unscrambled. After the background had been subtracted from each spectrum, the procedure used for unscrambling was essentially as described by Heath[1]. The specific procedure employed is described below.

Starting with the highest energy peak in the high energy spectrum the energy of this peak was determined. Then using a graph of the cave crystal resolution versus gamma-ray energy (prepared from Co^{60}, Ba^{133}, Zn^{65}, Mn^{54}, and Cr^{51} spectra obtained at the same geometry) the 1/2 width of this peak was found. Next a monoenergetic gamma source of energy as near as possible to this gamma was selected and a spectrum taken with the multi-channel analyzer to obtain a peak with the proper 1/2 width. To this peak portion of the spectrum a Compton distribution taken on the multi-channel analyzer was attached with the Compton edge and back scatter peak appropriate for the gamma-ray energy being synthesized. The energies of the Compton edge and back scatter peak were obtained from page 63 of the 1960 Nuclear Data Tables, Part 3, Nuclear Reaction Graphs (USAEC). In order to obtain the proper ratio of peak counts to total counts the Compton distributions had to be corrected for intensity since the energy of the gamma ray used for synthesis was not the same as the gamma ray being synthesized. The relationship used for this purpose was:

$$N_{c\gamma} = \frac{N_{p\gamma}\,(P_s)\,(1-P_\gamma)}{N_{ps}\,(P_\gamma)\,(1-P_s)}\,N_{cs}$$

---

[1]Heath, op. cit., p. 17.

PLATE XIV

SM+HE^3 (SM^{147} ENRICHED) SPECTRA FOR UNSCRAMBLING

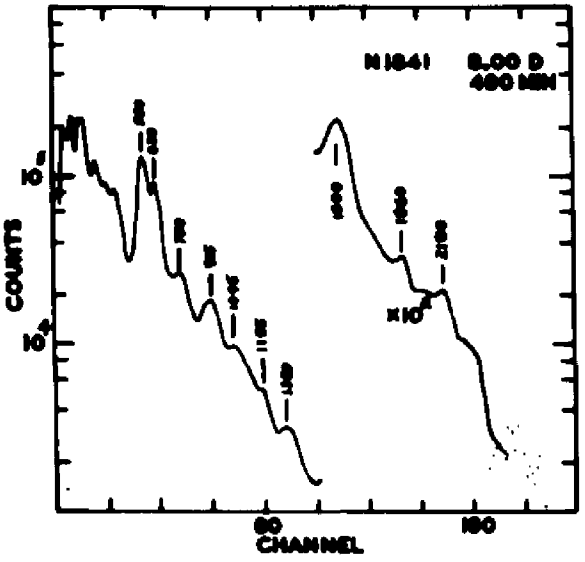

FIGURE 46. HIGH ENERGY SPECTRUM

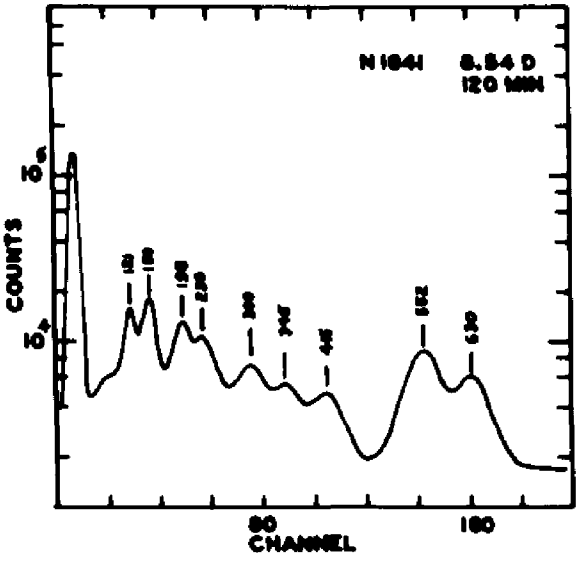

FIGURE 47. MEDIUM ENERGY SPECTRUM

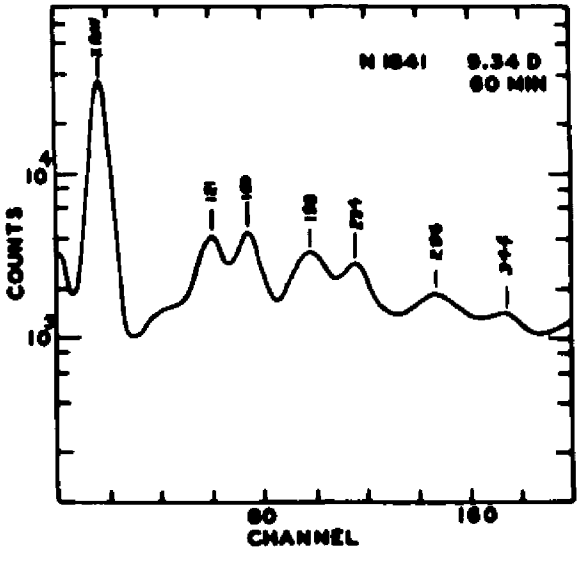

FIGURE 48. LOW ENERGY SPECTRUM

where $N_{c\gamma'}$ = Number of counts in one channel of the non-peak portion of the synthetic spectrum,

if $N_{p\gamma'}$ = Total number of counts in the gamma-ray peak on the spectra being synthesized,

N_{ps} = Total number of counts in the gamma-ray peak used for synthesis,

$P_s, P_{\gamma'}$ = Ratio of the number of counts in the gamma-ray peak to the total number of counts in the monoenergetic spectra for the synthesizing gamma and the synthesized gamma respectively.

and, N_{cs} = Number of counts in the corresponding channel x of the non-peak portion of the Compton spectrum used for synthesis.

The peak to total ratios, P_s and $P_{\gamma'}$, used in unscrambling were determined from a graph prepared for the O.S.U. cave crystal using monoenergetic gamma-ray spectra. Finally this synthetic, monoenergetic spectrum was subtracted channel by channel from the spectrum being unscrambled. This entire procedure was repeated until all spectra had been unscrambled down to the x ray with appropriate corrections on the Compton carry over for the different time intervals at which the spectra were taken.

The absolute number of counts due to a particular gamma ray ($N_{\gamma'}$) of energy (E) was calculated from:

$$N_{\gamma'} = N_{\gamma' p}(\epsilon_t P_{\gamma'} A)^{-1}$$

using peak to total ratio ($P_{\gamma'}$) curves, crystal efficiency (ϵ_t)

curves, the number of counts found in a particular unscrambled gamma-ray peak ($N_{\gamma p}$), and the correction for absorbers (A). Table 12 shows the results of unscrambling the three spectra.

9. RADIOACTIVE ISOTOPES IDENTIFIED IN SAMARIUM SAMPLES

Because of the high enrichment of Sm^{147} and the results observed with the Gadolinium samples only reactions involving Sm^{147} were expected to be significant. A search of the literature[26-37] for information on Gd^{147}, Gd^{148}, Gd^{149}, Eu^{147}, Eu^{148}, and Eu^{149} and comparison of the reported decay schemes with the data substantiated this assumption. Table 13 summarizes the gamma-ray energies and intensities reported. The notation which indicates gamma rays identified in this investigation is the same as that used in Table 8 for the Gadolinium samples. That is, the energies and intensities of observed gamma rays are listed and if identifiable from the cave crystal data marked with a gamma-ray number from Table 9. Of the gammas listed and not identified: S6 (2180), S15 (2080) and S19 (1185) are probably sum

---

[26] C.F. Schwerdtfeger et al., Nuclear Phys. 35, 168 (1962).
[27] B.S. Dzhelepov et al., Nuclear Phys. 30, 120 (1962).
[28] C.F. Schwerdtfeger et al., Phys. Rev. 125, 1641 (1926).
[29] K. Sugiyama, J. Phys. Soc. Japan 17, 264 (1962).
[30] B. Harmatz et al., Phys. Rev. 123, 1758 (1961).
[31] B.S. Dzhelepov et al., Nuclear Phys. 30, 110 (1962).
[32] A. Sorokin and K. Mitrofanov, Izvest. Akad. Nauk. USSR, Ser. Fiz. 25, 802 (1961).
[33] G. Groeffe and M. Nurmia, Ann. Acad. Sci. Fennicae Ser. A, VI-77, 1 (1961).
[34] O.K. Harling, Phys. Rev. 124, 1907 (1961).
[35] V.S. Shirley et al., Nuclear Phys. 4, 395 (1957).
[36] J.O. Rasmussen et al., Phys. Rev. 89, 33 (1953).
[37] H. J. Prask et al., Nuclear Phys. 30, 441 (1962).

TABLE 12

Sm + He^3(Sm^{147} ENRICHED) GAMMA RAYS FOUND BY UNSCRAMBLING CAVE CRYSTAL SPECTRA AT 9 DAYS

No.	E (keV)	N_{γ} p	N_{γ} (x10-4)	No.	E (keV)	N_{γ} p	N_{γ} (x10-4)
SPECTRUM DESCRIPTION: High Energy (H), T = 490 minutes, started at 8.015 days after bombardment. Gamma Energies Accurate to ±15 keV.							
1	2260	710	7.65 ± 7.8%	16	1065	31761	168.9 ± 4.7%
2	2150	1530	15.49 6.4%	17	1010	29395	146.8 4.4%
3	2040	1435	13.90 7.4%	18	940	51404	241.9 4.6%
4	1915	2408	22.13 6.0%	19	900	10388	46.7 8.7%
5	1800	2145	18.60 6.3%	20	885	49863	220.7 4.0%
6	1710	2457	20.35 8.2%	21	830	31893	132.3 4.7%
7	1650	3909	31.17 6.7%	22	775	72754	283.4 3.8%
8	1600	10875	84.89 4.4%	23	735	43279	160.2 6.2%
9	1525	6506	48.48 5.6%	24	705	38168	135.4 6.8%
10	1445	5011	34.91 6.4%	25	680	26308	90.6 8.6%
11	1370	6044	40.13 6.8%	26	650	73042	244.6 4.8%
12	1310	14130	90.12 4.5%	27	625	171645	545.4 4.0%
13	1230	8321	50.58 6.9%	28	595	155061	468.2 3.8%
14	1175	17117	100.3 5.1%	29	550	360387	1008. 3.5%
15	1120	17759	98.18 6.9%				
SPECTRUM DESCRIPTION: Medium Energy (M), T = 120 minutes, started at 8.542 days after bombardment. Gamma Energies Accurate to ±5 keV.							
27M	630	43136	137.8 ± 7.9%	35	340	19146	34.65 ± 6.6%
28M	597	54192	164.8 5.0%	36	320	9931	16.13 11. %
29M	540	83570	229.5 5.3%	37	293	30580	49.53 4.9%
30	518	24952	66.01 6.1%	38	264	5673	8.60 12. %
31	487	6995	17.08 9.5%	39	230	34753	18.81 5.2%
32	455	2846	6.57 15. %	40	195	51428	65.58 4.3%
33	412	18480	39.24 8.7%	41	148	75066	84.51 4.1%
34	388	19869	40.11 6.3%				
SPECTRUM DESCRIPTION: Low Energy (L), T = 60 minutes, started at 9.326 days after bombardment. Gamma Energies Accurate to ±2 keV.							
35L	344	10940	20.01 ± 6.9%	41	149	31311	36.47 ± 4.9%
37L	300	15284	25.31 6.1%	42	121	24742	26.19 5.2%
38L	278	4026	6.31 13. %	43	~80	1995	20.36 42. %
39L	230	17229	23.93 5.5%	44	x ray	293905	243.9 3.2%
40L	197	22513	28.84 5.4%				

TABLE 13

Sm + He^3(Sm^{147} ENRICHED) RADIOACTIVE ISOTOPES OF Gd AND Eu

Sm^{147} (97.8%) 1.3×10^{11}y α: 2.18 MeV	Sm^{148} (0.91%) Stable	Sm^{149} (0.51%) Stable
Eu^{147} 24d, E.C. γ: 76(28) 122(826) S27, A 198(1090) S27, A 600(398) } S26, A 680(562) } 800(290) S25, A 881(220) 900(---) 957(352) S24, P 1079(349) S28, P	Eu^{148} 58d, E.C. γ: 414(44) S11, A 551(172) S21, A 553(35) 631(163) S10, A 727(31.7) S22, P 870(13.5) S14, A 915(15.3) S 8, P 1020(14.4) S 7, P 1335(9.4) S20, A 1515(6.1) S18, A 1600(14.7) S17, A	Eu^{149} 106d, E.C. γ: 22.5(150) 73.0(4) S2, P 178(7) 208(---) 255(210) ? } S3, A 277(1190) } 281 ? 328(1296) S4, A 350(74) S5, P 506(122) 529(98) 536(---) 558(---)
Gd^{147} 35h, E.C. γ: 229(240) S37, A 261 S42, A 370(40) S38, P 396(100) S39, A 485 549 560(23) S40, A 617 625(50) S36, A 703 755 766(88) S35, A 778 787 860 896(94) S34, P 932 S41, P 995 1130 S43, P 1330 S44, A	Gd^{148} >35y α: 3.16 MeV	Gd^{149} 9.5d, E.C. γ: 150(190) S29,A 273(18) 299(103) S29,A 347(100) S29,A 461(6) 497(9) 517 (22) 535 646(9) 660(5) 750(45) 790(37) 870(3) 933(5) 940(15)

peaks caused by the 2202, 2097 and 1182 keV levels recently reported by Schwerdtfeger[28] in Eu^{148}. S45 (1590) and S46 (1790) are also possibly sum peaks associated with the 1556 and 1742 keV levels reported for Gd^{147}. However, the prominence of these peaks (see Plate IX) and the existence of other gamma rays (S47 (1960), S48 (2180), and S49 (2260)) points to the possibility of higher energy levels associated with Gd^{147}. The data obtained in this investigation is insufficient to draw any definite conclusions. The decay half-lives and energy shift to the x ray observed on the x-ray crystal also gave evidence for the presence initially of Gadolinium isotopes and finally Europium isotopes decaying by electron capture. The results from the solid state alpha detector confirm the existence of alpha particle activity in the early stages of decay, while a comparison of the unscrambled photon spectral intensities is in good agreement for all the major transitions.

Additional evidence for the presence of the isotopes Gd^{147}, Gd^{149}, Eu^{147}, Eu^{148}, and Eu^{149} is provided by the well crystal and the coincidence data. Table 14 compares, in part, the sums and coincidences expected from the reported decay schemes with the experimental data obtained in this investigation and presented in Tables 10 and 11, and Plate XI. Because of the complexity of the spectra only the more intense transitions have been considered. The general agreement with reported data is good. However, the sum data taken at 142 days has a low energy structure that is not entirely compatible with the reported decay schemes for Eu^{149}. At this time the predominant activities

---

[28] C.F. Schwerdtfeger, op. cit., p. 164.

TABLE 14

A COMPARISON OF SUM AND COINCIDENCE DATA WITH REPORTED ENERGY LEVEL DIAGRAMS OF Eu^{147}, Eu^{148}, Eu^{149}, Gd^{147} AND Gd^{149}

Description of Isotope	Partial List of Gamma-Ray Coincidences		Partial List of Gamma-Ray Sum Peaks	
	Gamma Ray	Coincident Gamma Rays	Expected	Observed
Gd^{147}, 35h, E.C. Reported by: See Ref 35, 36	229	396, 766, 896, 1330	625	Yes
	261		766	Probable
	370	396, 560, 625	930	Yes
	396	229, 370, 932	995	Yes
	560	370, 766	1125	Yes
	625	370, 932	1557-1559	Probable
Gd^{149}, 9.5d, E.C. Reported by: See Ref 37	150	347	423	Probable
	299	347	497	Probable
	347	150, 299	646	---
Eu^{147} 23.6d E.C. Reported by: See Ref 26, 27	122	680, 957	198	Yes
	198	600	676	Yes
	800	None	776, 800	Probable
	1079	None	900, 957	Probable
Eu^{148} 58d, E.C. Reported by: See Ref 28, 29	414	553, 631	967	Yes
	551	631, 1335	1045	Yes
	631	414, 551, 726, 915, 1020, 1515, 1600	1182	Yes
			1357	Probable
	726	631, 870	1596	Yes
			1651	Probable
			1886	Yes
			2146	Yes
			2231	Yes
Eu^{149} 106d, E.C. Reported by: See Ref 31, 32, 34	No conclusive results as coincidence data was not taken sufficiently long after bombardment.		251	Yes
			278, 281	Yes
			328	Yes
			529	Probable
			558	Probable

should be mainly Eu^{148} and Eu^{149} (with some Eu^{147}). Inspection of Plate X, Figure 31, bears out this conclusion. The sum peaks at 78 and 122 keV cannot be accounted for using any of the reported decay schemes for Eu^{149}. The gamma S1 ($\sim$ 58 keV) listed in Table 9, as yet unaccounted for, may be involved in these sum peaks. It appears that the decay of Eu^{149} merits more investigation.

In summary, as a result of the He^3 bombardment of the Samarium sample the isotopes found to be present and with decay schemes and intensities in general agreement with previously reported data were:

Gd^{147} ($T^{\frac{1}{2}} = 35h$)[35] Eu^{147} ($T^{\frac{1}{2}} = 26.4 \pm 2.0d$)

Gd^{149} ($T^{\frac{1}{2}} = 9.5 \pm 0.3d$)[37] Eu^{148} ($T^{\frac{1}{2}} = 55.9 \pm 2.0d$)

Eu^{149} ($T^{\frac{1}{2}} = 106 \pm 2d$)[34]

10. RELATIVE AMOUNTS OF Gd AND Eu ISOTOPES PRODUCED IN SAMARIUM SAMPLE

Since the gamma-ray intensities for the isotopes of Gd and Eu have all been reported it is possible to use the data obtained from the unscrambling spectra to determine the proportions of each present at the end of the bombardment. The procedure used to determine the original isotopic amounts was, first, to derive the relationship between the number of atoms at bombardment off and the number which decay during the time interval over which the spectra was taken. Secondly, to relate the number of atoms decaying to the number of gamma rays counted in a particular transition during this period; and

---

[35] V.S. Shirley et al., op. cit., p. 395.
[37] H.J. Prask, op. cit., p. 441.
[34] O.K. Harling, op. cit., p. 1907.

finally, selecting the most suitable gamma rays from the unscrambling spectra, use these relationships to calculate the number of atoms present at the end of the bombardment. This information can then be directly related to the relative cross-sections for the reaction channels occuring in the $He^3 + Sm^{147}$ reaction.

a. Decay Relationships for Gd^{147}, Gd^{149}, Eu^{147}, Eu^{148}, and Eu^{149}.

The decay systematics for the isotopes of interest, where the long half-life isotopes can be neglected, are

$$\begin{aligned}
&Gd^{147}(C) \xrightarrow[35h]{} Eu^{147}(A_c) \xrightarrow[23.6 \pm 1.0d]{} Sm^{147}(E), \\
&Gd^{149}(H) \xrightarrow[9.5 \pm 0.3d]{} Eu^{149}(K_h) \xrightarrow[106 \pm 2d]{} Sm^{149}(L), \\
&Eu^{147}(A) \xrightarrow[23.6 \pm 1.0d]{} Sm^{147}(B), \\
&Eu^{148}(F) \xrightarrow[58 \pm 3d]{} Sm^{148}(G), \\
\text{and} \quad &Eu^{149}(K) \xrightarrow[106 \pm 2d]{} Sm^{149}(L).
\end{aligned} \tag{10-1}$$

The letters enclosed in brackets identify a particular isotope. Thus, the letters C, H, A, F, and K each represent the number of atoms of an isotope present at a time t (after bombardment) due to those present at t = 0 (end of bombardment); while the subscripted letters A_c, and K_h represent the number of atoms of an isotope present at time t formed by decay. Using equations (10-1), we can write the decay equations

$$\begin{aligned}
&C = C_o \exp(-\lambda_c t), \\
&H = H_o \exp(-\lambda_h t), \\
&A = A_o \exp(-\lambda_a t), \\
&F = F_o \exp(-\lambda_f t), \\
\text{and} \quad &K = K_o \exp(-\lambda_k t),
\end{aligned} \tag{10-2}$$

for the primary formation of each isotope; and

$$A_c = C_o(\lambda_c/\lambda_a - \lambda_c)\left[\exp(-\lambda_c t) - \exp(-\lambda_a t)\right] \qquad (10\text{-}3)$$

$$K_h = H_o(\lambda_h/\lambda_k - \lambda_h)\left[\exp(-\lambda_h t) - \exp(-\lambda_k t)\right]$$

for the formation of isotopes due to decay. In the above equations a "o" subscript identified the number of atoms present at $t = 0$, and the symbol λ is the decay constant.

In order to determine the number of atoms decaying during a particular counting period, if $X(t_s)$ is the number of atoms of isotope X present at the start of the period and $X(t_e)$ is the number present at the end of the period then the number of atoms which decayed in this period is

$$\Delta X = X(t_s) - X(t_e). \qquad (10\text{-}4)$$

Now, if we define

$$e(X) \equiv \exp(-\lambda_x t_s) - \exp(-\lambda_x t_e)$$

and substitute the appropriate equations (10-2) and (10-3) into equations (10-4) we obtain:

$$\Delta C = C_o\, e(C),$$

$$\Delta H = H_o\, e(H),$$

$$\Delta A = A_o\, e(A) C_o(\lambda_c/\lambda_a - \lambda_c)\left[e(C) - e(A)\right], \qquad (10\text{-}5)$$

$$\Delta F = F_o\, e(F),$$

and $$\Delta K = K_o\, e(K)\, H_o(\lambda_h/\lambda_k - \lambda_h)\left[e(H) - e(K)\right].$$

Solving then for the number of atoms present at $t = 0$ gives

$$C_o = \Delta C/e(C)$$

$$H_o = \Delta H/e(H) \qquad (10\text{-}6)$$

$$A_o = \Delta A/e(A) - \Delta C(\lambda_c/\lambda_a - \lambda_c)\left[1/e(A) - 1/e(C)\right]$$

$$F_o = \Delta F/e(F)$$

and $$K_o = \Delta K/e(K) - \Delta H(\lambda_h/\lambda_k - \lambda_h)\left[1/e(K) - 1/e(H)\right]$$

respectively, as the number of atoms of each isotope present at t 0.

b. The Relationship between Photon Intensities and Decay Equations

To relate equations (10-6) to the experimental data, the number of atoms decaying in a counting period (ΔX) has to be related to the absolute number of gamma rays (P_γ) counted in the same period.

Let $\Delta G(i,n)$ represent the number of transitions of energy $E_i - E_n$, where E_i is the initial energy level and E_n is the terminal energy level, occuring in the counting interval $(t_e - t_s)$. Since converted gamma rays are not detected, we suppose a converted fraction $Q(i,n)$. Now the NaI(Tl) crystal detects (with corrections for absorption, solid angle and efficiency), in this same time interval, a number of gamma-ray transitions $N_\gamma(i,n)$ where

$$\Delta G(i,n) = \frac{N_\gamma(i,n)}{Q(i,n)} . \qquad (10\text{-}7)$$

Now, to find the total number of atoms decaying in the counting period (ΔX) we must relate it to $\Delta G(i,n)$. This can be done by referring to the decay scheme of the particular isotope of interest. Consider then the generalized level scheme:

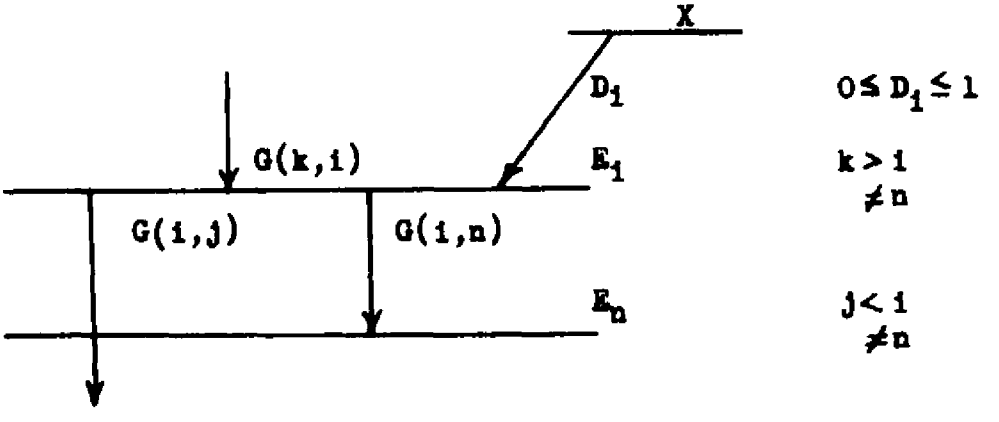

We note that level E_i is fed by direct transitions, with the potential number of transitions due to this source being $D_i \Delta X$, and by other transitions $\Delta G(k,i)$ resulting in potential additional transitions equal to $\sum_k \Delta G(k,i)$. Also transitions $\Delta G(i,j)$ deplete the level E_i so we have a potential loss of counts of $\sum_j \Delta G(i,j)$. Thus, the relationship between the number of atoms ΔX decaying in the period $t_e - t_s$ and the number of photons $N_\gamma(i,n)$ counted for a particular transition $G(i,n)$ is (10-8)

$$\Delta X = \frac{1}{D_i}\left[\frac{N_\gamma(i,n)}{Q(i,n)} - \sum_{k>i}\frac{N_\gamma(k,i)}{Q(k,i)} + \sum_{j<i}\frac{N_\gamma(i,j)}{Q(i,j)}\right]$$

All quantities in this equation can be determined using reported decay systematics and the unscrambling results obtained from Table 12. Once the ΔX's are known these numbers are substituted into equations (10-6) and the original amounts of each isotope can, in principle, be calculated.

c. Calculation of the Amounts of Gd and Eu Isotopes Produced.

Extensive examination of the unscrambling results and decay schemes showed that the most suitable procedure to follow in separating the isotopes was to remove them in this order:

1. Gd^{149} using the 150 and 299 keV transition data reported by Prask et al.[37]
2. Gd^{147} using the 229 keV transition data reported by Shirley et al. [35]

---

[37] Prask, op. cit., p. 441.
[35] Shirley, op. cit., p. 395.

3. Eu^{148} using the 413.7, 550.7-553.2, 630.7 keV transition data reported by Schwerdtfeger et al.[28]
4. Eu^{147} using the 121.8 and 198.1 keV transition data reported by Schwerdtfeger et al.[26]
5. Eu^{149} using the 277.2 and 327.7 keV transition data reported by Harmatz et al.[30]

The gamma-ray counts necessary to make these subtractions were selected from the unscrambling data and are listed in Table 15. Using this data and transition data obtained from the literature in conjunction with equations (10-6) and (10-8) the number of atoms of each isotope present of the time the bombardment ceased were found to be:

Gd^{149}; $K_o = (5.8 \pm 1.2) \times 10^8$

Gd^{147}; $C_o = (10.9 \pm 1.6) \times 10^8$

Eu^{148}; $F_o = (10.2 \pm 3.9) \times 10^8$

Eu^{147}; $A_o = (12 \pm 6) \times 10^8$

Eu^{149}; $K_o = (22 \pm 11) \times 10^8$

---

[28] C.F. Schwerdtfeger et al, op. cit., p. 164.
[26] C.F. Schwerdtfeger et al, op. cit., p. 168.
[30] B. Harmatz et al, op. cit., p. 1758.

TABLE 15

ISOTOPE SEPARATION DATA

No	E(keV)	$N_{\gamma t}$ (x10^{-4})	Isotope (λ min^{-1}) and Energy (keV)
High Energy (H): t_s = 1.1541x10^4 min, t_e = 1.2031x10^4 min.			
27	625	545.4 ± 4.0%	Eu-148(λ_f = 8.31x10^{-6} ± 1.9%); 630.7
28	550	1008.0 3.5%	Eu-148; 550.7, 553.2
Medium Energy (M): t_s = 1.2300x10^4 min, t_e = 1.2420x10^4 min.			
27M	630	137.8 ± 7.9%	Eu-148; 630.7
28M	540	229.5 5.3%	Eu-148; 550.7, 553.2
33	412	39.24 8.7%	Eu-148; 413.7
36	320	16.13 11.0%	Eu-149; (λ_k = 4.54x10^{-6} ± 1.9%); 327.7
37	293	49.53 4.9%	Gd-149; (λ_h = 5.07x10^{-5} ± 3.2%); 299
38	264	8.56 12.0%	Eu-149; 277.2
39	230	48.81 5.2%	Gd-147; (λ_c = 3.30x10^{-4} ± 3.0%); 229
40	195	65.58 4.3%	Eu-147; (λ_a = 2.04x10^{-5} ± 4.4%); 198.1
41	148	84.51 4.1%	Gd-149; 149
Low Energy (L): t_s = 1.340x10^4 min, t_e = 1.3490 min.			
37L	300	25.31 ± 6.1%	Gd-149; 300
38L	278	6.31 13.0%	Eu-149; 277.2
39L	230	23.93 5.5%	Gd-147; 229
40L	197	28.84 5.4%	Eu-147; 198.1
41L	149	35.57 4.9%	Gd-149; 149
42	121	26.19 5.2%	Eu-147; 121.8

IV. CONCLUSIONS

1. GADOLINIUM 152

The low enrichment of Gd^{152} resulted in the production of a number of unrelated isotopes which complicated the gamma spectra. Obviously, higher enrichments of the isotope of interest are desirable for bombardments with He^3. Nevertheless, this investigation has established the background data against which studies of Dy^{152} and Dy^{153} can and should be made.

In comparison of this data with reported data it was found that the alpha activity supported the long half-life assignment by Macfarlane for Dy^{154}. All gamma activity could be correlated except the 31.2 keV gamma ray which has the same energy as that reported in the decay of Tb^{155}. However, the half-life of 2.3 days for the radionuclide which emits the gamma ray and the magnitude of the intensity support the assignment to Tb^{153}.

The only completely new information is the reported 145 keV gamma ray. The half-life of the observed intensity is about 270 days. No definite assignment can be made at present since longer term information is needed.

2. SAMARIUM 147

The high enrichment of Sm^{147} made possible the quantitative analysis of this sample and a high degree of correlation with the literature. It also appears that further investigation of the short

half-life activities produced by He^3 will yield significant information on Gd^{147} gamma activities and intensities.

In comparison of this data with that published, good agreement was obtained. The half-lives of Eu^{147} (26.4d) and Eu^{148} (55.9d) are in good agreement with those previously reported. The decay data on Eu^{149} supports the 106 day half-life reported by Harling[34], but there also appears to be low energy gamma structure associated with the decay of Eu^{149} that has not been reported.

Using the published decay systematics and data obtained in this investigation it was possible to calculate the cross section ratios for five of the six reactions listed earlier. It was found that the Sm^{147} + He^3 reactions

(He^3,T), (He^3,d), (He^3,p), (He^3,n), $(He^3,3n)$

were respectively, in the ratios

$(12 \pm 6) : (10.2 \pm 3.9) : (22 \pm 11) : (5.8 \pm 1.2) : (10.9 \pm 1.6)$.

The bombardment energy for incident particles was 15 MeV. An estimate of the cross section for the reaction producing Eu^{149} was made and found to be of the order of 5×10^{-27} cm^2.

---

[34] Harling, op. cit., p. 1907.

AUTOBIOGRAPHY

I, Raymond Hal Kelley, was born in Roscoe, Montana, July 10, 1922. I received my elementary school education at Mystic Lake, Montana, and attended high school at Absarokee, Montana. I obtained a B.S. in Engineering Physics at Montana State College in 1950.

I next taught electronics for two and one-half years at Ellington Air Force Base. I earned the M.Sc. degree in Physics from Ohio State University in 1955 and thereafter was engaged in research in nuclear and solid state physics at the Aeronautical Research Laboratory, Wright-Patterson Air Force Base, Ohio. Returning to Ohio State University in 1960, I continued my work in physics toward a Doctor of Philosophy degree.

I am currently an Assistant Professor of Physics at the United States Air Force Academy, Colorado.